Comput Mech (2007) 40:261–279
DOI 10.1007/s00466-006-0096-z

ORIGINAL PAPER

A new high-order accurate continuous Galerkin method for linear elastodynamics problems

Alexander V. Idesman

Received: 11 February 2006 / Accepted: 15 June 2006 / Published online: 17 August 2006

Abstract A new high-order accurate time-continuous Galerkin (TCG) method for elastodynamics is suggested. The accuracy of the new implicit TCG method is increased by a factor of two in comparison to that of the standard TCG method and is one order higher than the accuracy of the standard time-discontinuous Galerkin (TDG) method at the same number of degrees of freedom. The new method is unconditionally stable and has controllable numerical dissipation at high frequencies. An iterative predictor/multi-corrector solver that includes the factorization of the effective mass matrix of the same dimension as that of the mass matrix for the second-order methods is developed for the new TCG method. A new strategy combining numerical methods with small and large numerical dissipation is developed for elastodynamics. Simple numerical tests show a significant reduction in the computation time (by 5–25 times) for the new TCG method in comparison to that for second-order methods, and the suppression of spurious high-frequency oscillations.

1 Introduction

Most finite element procedures for elastodynamics problems are based upon semi-discrete methods [7–9,22,23,26–28]. For these methods, the application of finite elements in space to linear elastodynamics problems leads to a system of ordinary differential equations in time

$$\boldsymbol{M}\ddot{\boldsymbol{U}} + \boldsymbol{C}\dot{\boldsymbol{U}} + \boldsymbol{K}\boldsymbol{U} = \boldsymbol{R}, \tag{1}$$

which are in turn discretized by finite difference methods for ordinary differential equations. Here $\boldsymbol{M}, \boldsymbol{C}, \boldsymbol{K}$ are the mass, damping and stiffness matrices, respectively, $\boldsymbol{U}(t)$ is the vector of the nodal displacement, $\boldsymbol{R}(t)$ is the vector of the nodal load. Among semi-discrete methods, second-order accurate methods, such as the Houbolt method, the Newmark method, the Wilson-θ method, the Park method, and the HHT-α method, are the most frequently used. Zienkiewich and coworkers (see [27, 28]) have developed and analyzed a set of algorithms, called the unified set of a single step method, based on the application of the weighted residual method to the equation of motion. Many of the classical finite difference schemes mentioned above are particular cases of the unified set. High accuracy can be obtained by using higher-order interpolation polynomials. However, the high-order accurate method suggested in [27,28] is not unconditionally stable for elastodynamics.

Recently, new high-order accurate methods with a step-by-step time integration scheme have been developed for elastodynamics (see [1,2,4,6,11–13,15–17,21, 24,25] and others). Most of them are based on semi-discrete equations with the polynomial time approximations of unknown functions. The polynomial coefficients are derived with the use of different approaches such as TCG and TDG methods, weighted residual methods, collocation methods and others. The ultimate goal in the development of high-order accurate methods is to construct an unconditionally stable method with

A. V. Idesman (✉)
Department of Mechanical Engineering,
Texas Tech University, Lubbock, TX 79409-1021, USA
e-mail: alexander.idesman@coe.ttu.edu

controllable numerical dissipation that is much more computationally effective than known second-order methods. Because many high-order accurate methods require the solution of a large system of equations (much larger than the system for second-order methods), the development of effective iterative predictor/multi-corrector solvers is an important component of the method.

The focus of this paper is the development of a new high-order accurate method for elastodynamics. The new method is based on a modified continuous Galerkin formulation and polynomial time approximations of displacements and velocities. Initial conditions are strongly enforced. For linear, quadratic and third-order polynomial time approximations the method has the second, fourth and sixth order of accuracy, respectively. It means that the accuracy of the new implicit TCG method is increased by a factor of two in comparison to that of the standard TCG method [3] and is one order higher than the accuracy of the standard TDG method [12–15,17,18] (and the high-order accurate methods suggested in [6,21]) at the same number of degrees of freedom. The new method is unconditionally stable and has controllable numerical dissipation at high frequencies. An iterative predictor/multi-corrector solver that includes the factorization of the effective mass matrix of the same dimension as that of the mass matrix for the second-order methods is developed for the new TCG method. This iterative predictor/multi-corrector solver requires only a few iterations in order to reach the accuracy of direct solvers. For example, two iterations are needed for the fourth-order of accuracy and three iterations for the sixth-order of accuracy. The suggested predictor/multi-corrector solver is much more effective than those developed for high-order methods. For example, the predictor/multi-corrector solver suggested in [21] for modified Nørsett methods requires one iteration in order to improve the order of accuracy by one. The predictor/multi-corrector solver for the TDG method suggested in [17] is only conditionally stable for third-order time approximations and is studied for problems without damping. Many different iterative solvers were developed for the TDG method but only for the linear time approximations (see [1,2,4,5,18–20,25] and others). Simple 1-D numerical tests show that even with a direct solver the new TCG method reduces the computation time by 5–25 times in comparison to that of the second-order methods and is much faster than the TDG method. Because the numerical error is usually greater for 2-D and 3-D problems and is accumulated during the time integration, the new technique should be even more effective for multi-dimensional problems.

It is necessary to note that known semi-discrete and TDG methods lead to a spurious high-frequency response for wave propagation problems [4,10,15,20,24], especially with non-uniform meshes (see Fig. 8b below). However, numerical results considered in the paper show that for the new TCG method, the spurious oscillations can be excluded due to controllable numerical dissipation. In the paper we propose a new general strategy that allows the effective use of numerical methods with zero or small numerical dissipation for wave propagation problems. The idea consists in the combination of numerical methods with small and large numerical dissipation. The basic computations, especially for a long-term integration, can be made with a high-order method with zero or very small numerical dissipation. It means that all modes are integrated very accurately. Then, in order to damp out high modes, a method with large numerical dissipation can be used for a number of last time increments or as a post-processor. This method can be considered as a filter of high modes. An example of the application of the new strategy with the new TCG method shows the effectiveness of the new approach.

2 Variational formulation of elastodynamics

2.1 Weak and discrete formulations of elastodynamics based on continuous Galerkin time-stepping methods

For the derivation of weak and discrete formulations of elastodynamics, the so-called two-field formulation will be used. For this aim the finite element equations (1) can be rewritten as follows:

$$\boldsymbol{M}\dot{\boldsymbol{V}} + \boldsymbol{C}\boldsymbol{V} + \boldsymbol{K}\boldsymbol{U} = \boldsymbol{R}, \qquad \boldsymbol{V} = \dot{\boldsymbol{U}}, \tag{2}$$

where $\boldsymbol{V}(t)$ is the vector of the nodal velocity. Eq. (2) are a system of ordinary differential equations. For the continuous Galerkin time-stepping method, we introduce a partition of the whole time interval $[0,\ T]$ in a not necessarily uniform fashion by $0 = t_0 < t_1 < \cdots < t_n < \cdots < t_N$ and define the time intervals $J_n = (t_{n-1}, t_n], n = 1, \ldots, N$, where $t_N = T$. A weak formulation of elastodynamics for any time interval J_n can be derived from Eq. (2) as follows:

$$\int_{J_n} (\bar{\boldsymbol{v}}^T + a\dot{\bar{\boldsymbol{v}}}^T)[\boldsymbol{M}\dot{\boldsymbol{V}} + \boldsymbol{C}\boldsymbol{V} + \boldsymbol{K}\boldsymbol{U} - \boldsymbol{R}]\,\lambda_1(t)\,\mathrm{d}t = 0,$$

$$\int_{J_n} (\bar{\boldsymbol{u}}^T + a\dot{\bar{\boldsymbol{u}}}^T)\ (\dot{\boldsymbol{U}} - \boldsymbol{V})\ \lambda_2(t)\,\mathrm{d}t = 0, \tag{3}$$

where $\bar{\boldsymbol{u}}(t)$ and $\bar{\boldsymbol{v}}(t)$ are the trial vector functions depending on time t; a is the scalar coefficient and has the dimension of time (e.g. s); $\lambda_1(t)$ and $\lambda_2(t)$ are the weighting scalar functions depending on time t only. At time t_{n-1} nodal displacements and velocities $\boldsymbol{U}(t_{n-1})$ and $\boldsymbol{V}(t_{n-1})$ are known from the solution for the previous time interval J_{n-1}, or from the initial conditions, and $\bar{\boldsymbol{u}}(t_{n-1}) = \bar{\boldsymbol{v}}(t_{n-1}) = \boldsymbol{0}$. For any time interval J_n a local time $t^* = t - t_{n-1}$ can be introduced. Time t^* varies from 0 to Δt ($\Delta t = t_n - t_{n-1}$). For convenience, for all derivations for time intervals J_n, the local time t^* will be used. However, in order to simplify notations the local time will be designated as t. The advantages of using additional scalar functions $\lambda_1(t)$ and $\lambda_2(t)$ were considered in the author's paper (A. V. Idesman, submitted). At special polynomial approximations of these functions, they do not affect the accuracy of the numerical algorithm but allow control of additional algorithmic characteristics, e.g., the spectral radii (A. V. Idesman, submitted). In this paper we assume for simplicity that $\lambda_1(t) = \lambda_2(t) = 1$. The numerical algorithm with polynomial functions $\lambda_1(t)$ and $\lambda_2(t)$ can be derived without any difficulties.

To get a discrete formulation from Eq. (3) the following time polynomial approximations of the order n for any time interval J_n will be used for $\boldsymbol{U}(t), \boldsymbol{V}(t), \bar{\boldsymbol{u}}(t)$ and $\bar{\boldsymbol{v}}(t)$

$$\begin{aligned}
\boldsymbol{U}(t) &= \boldsymbol{U}_0 + \boldsymbol{U}_1 t + \boldsymbol{U}_2 t^2 + \cdots + \boldsymbol{U}_n t^n,\\
\boldsymbol{V}(t) &= \boldsymbol{V}_0 + \boldsymbol{V}_1 t + \boldsymbol{V}_2 t^2 + \cdots + \boldsymbol{V}_n t^n,\\
\bar{\boldsymbol{u}}(t) &= \bar{\boldsymbol{u}}_0 + \bar{\boldsymbol{u}}_1 t + \bar{\boldsymbol{u}}_2 t^2 + \cdots + \bar{\boldsymbol{u}}_n t^n,\\
\bar{\boldsymbol{v}}(t) &= \bar{\boldsymbol{v}}_0 + \bar{\boldsymbol{v}}_1 t + \bar{\boldsymbol{v}}_2 t^2 + \cdots + \bar{\boldsymbol{v}}_n t^n,
\end{aligned} \tag{4}$$

where $\boldsymbol{U}_0$ and $\boldsymbol{V}_0$ are the known initial displacement and velocity, $\boldsymbol{U}_1, \ldots, \boldsymbol{U}_n$ and $\boldsymbol{V}_1, \ldots, \boldsymbol{V}_n$ are unknown vectors to be determined, $\bar{\boldsymbol{u}}_0 = \bar{\boldsymbol{v}}_0 = \boldsymbol{0}$, and $\bar{\boldsymbol{u}}_1, \ldots, \bar{\boldsymbol{u}}_n$ and $\bar{\boldsymbol{v}}_1, \ldots, \bar{\boldsymbol{v}}_n$ are trial vectors. When Eq. (4) is inserted into Eq. (3), the final discrete system of algebraic equations for unknowns $\boldsymbol{U}_1, \ldots, \boldsymbol{U}_n$ and $\boldsymbol{V}_1, \ldots, \boldsymbol{V}_n$ is derived as follows:

$$\begin{aligned}
&(\boldsymbol{M}\boldsymbol{V}_1 + \boldsymbol{C}\boldsymbol{V}_0 + \boldsymbol{K}\boldsymbol{U}_0)\left(\frac{\Delta t}{1+k} + a\right)\\
&\quad + (2\boldsymbol{M}\boldsymbol{V}_2 + \boldsymbol{C}\boldsymbol{V}_1 + \boldsymbol{K}\boldsymbol{U}_1)\left(\frac{\Delta t}{2+k} + \frac{ak}{k+1}\right)\Delta t\\
&\quad + \cdots + (n\boldsymbol{M}\boldsymbol{V}_n + \boldsymbol{C}\boldsymbol{V}_{n-1} + \boldsymbol{K}\boldsymbol{U}_{n-1})\\
&\quad \times \left(\frac{\Delta t}{n+k} + \frac{ak}{n+k-1}\right)\Delta t^{n-1}\\
&\quad + (\boldsymbol{C}\boldsymbol{V}_n + \boldsymbol{K}\boldsymbol{U}_n)\left(\frac{\Delta t}{n+k+1} + \frac{ak}{n+k}\right)\Delta t^n\\
&= \boldsymbol{R}_k, \quad k = 1, 2, \ldots, n
\end{aligned} \tag{5}$$

$$\begin{aligned}
&(\boldsymbol{U}_1 - \boldsymbol{V}_0)\left(\frac{\Delta t}{1+k} + a\right)\\
&\quad + (2\boldsymbol{U}_2 - \boldsymbol{V}_1)\left(\frac{\Delta t}{2+k} + \frac{ak}{k+1}\right)\Delta t\\
&\quad + \cdots + (n\boldsymbol{U}_n - \boldsymbol{V}_{n-1})\left(\frac{\Delta t}{n+k} + \frac{ak}{n+k-1}\right)\Delta t^{n-1}\\
&\quad - \boldsymbol{V}_n\left(\frac{\Delta t}{n+k+1} + \frac{ak}{n+k}\right)\Delta t^n\\
&= \boldsymbol{0}, \quad k = 1, 2, \ldots, n
\end{aligned} \tag{6}$$

where

$$\boldsymbol{R}_k = \frac{1}{\Delta t^k}\int_0^{\Delta t} \boldsymbol{R}(t)(t^k + akt^{k-1})\,\mathrm{d}t. \tag{7}$$

This procedure can be considered as the application of the continuous Galerkin method to the system (2). Eqs. (5) and (6) represent a system of $2n$ algebraic equations with $2n$ unknown vectors $\boldsymbol{U}_1, \ldots, \boldsymbol{U}_n$ and $\boldsymbol{V}_1, \ldots, \boldsymbol{V}_n$. It is necessary to note that the system of n equations (6) can be analytically solved separately from the system (5); i.e., unknown vectors $\boldsymbol{V}_1, \ldots, \boldsymbol{V}_n$ can be expressed in terms of unknown vectors $\boldsymbol{U}_1, \ldots, \boldsymbol{U}_n$. Then the final system of equations (5) and (6) can be reduced to the system of only n equations with unknown vectors $\boldsymbol{U}_1, \ldots, \boldsymbol{U}_n$. Let us consider the derivation of the final system of equations for $n = 1, n = 2$ and $n = 3$ in detail. For the higher number of n the derivation is similar to these cases.

2.2 Linear time approximations ($n = 1$)

For the linear approximations of vectors $\boldsymbol{U}(t), \boldsymbol{V}(t), \bar{\boldsymbol{u}}(t)$ and $\bar{\boldsymbol{v}}(t)$, Eq. (4) can be rewritten as follows:

$$\begin{aligned}
&\boldsymbol{U}(t) = \boldsymbol{U}_0 + \boldsymbol{U}_1 t, \quad \boldsymbol{V}(t) = \boldsymbol{V}_0 + \boldsymbol{V}_1 t,\\
&\bar{\boldsymbol{u}}(t) = \bar{\boldsymbol{u}}_0 + \bar{\boldsymbol{u}}_1 t, \quad \bar{\boldsymbol{v}}(t) = \bar{\boldsymbol{v}}_0 + \bar{\boldsymbol{v}}_1 t.
\end{aligned} \tag{8}$$

Then from Eq. (6) we get

$$(\boldsymbol{U}_1 - \boldsymbol{V}_0)\left(\frac{\Delta t}{2} + a\right) - \boldsymbol{V}_1\left(\frac{\Delta t}{3} + \frac{a}{2}\right)\Delta t = \boldsymbol{0} \tag{9}$$

or

$$\boldsymbol{V}_1 = \frac{3(\Delta t + 2a)}{\Delta t(2\Delta t + 3a)}\boldsymbol{U}_1 - \frac{3(\Delta t + 2a)}{\Delta t(2\Delta t + 3a)}\boldsymbol{V}_0. \tag{10}$$

At $n = 1$ Eq. (5) reduces to

$$\begin{aligned}
&(\boldsymbol{M}\boldsymbol{V}_1 + \boldsymbol{C}\boldsymbol{V}_0 + \boldsymbol{K}\boldsymbol{U}_0)\frac{\Delta t + 2a}{2}\\
&\quad + (\boldsymbol{C}\boldsymbol{V}_1 + \boldsymbol{K}\boldsymbol{U}_1)\frac{2\Delta t + 3a}{6}\Delta t = \boldsymbol{R}_1.
\end{aligned} \tag{11}$$

By the insertion of Eq. (10) into Eq. (11), the following system can be obtained

$$\left(\boldsymbol{M} + a_1\boldsymbol{C} + a_1^2\boldsymbol{K}\right)\boldsymbol{U}_1 = -a_1\boldsymbol{K}\boldsymbol{U}_0 + \boldsymbol{M}\boldsymbol{V}_0 + a_2\boldsymbol{R}_1, \tag{12}$$

where

$$a_1 = \frac{\Delta t(2\Delta t+3a)}{3(\Delta t+2a)}, \quad a_2 = \frac{2(2\Delta t+3a)\Delta t}{3(\Delta t+2a)^2},$$
$$\boldsymbol{R}_1 = \frac{1}{\Delta t}\int_0^{\Delta t}\boldsymbol{R}(t)(t+a)\,\mathrm{d}t. \tag{13}$$

The vector $\boldsymbol{U}_1$ can be found from Eq. (12), then the vector $\boldsymbol{V}_1$ can be calculated from Eq. (10).

2.3 Quadratic time approximations ($n = 2$)

For the quadratic approximations of vectors $\boldsymbol{U}(t), \boldsymbol{V}(t)$, $\bar{\boldsymbol{u}}(t)$ and $\bar{\boldsymbol{v}}(t)$, Eq. (4) can be rewritten as follows:

$$\begin{aligned}
&\boldsymbol{U}(t) = \boldsymbol{U}_0 + \boldsymbol{U}_1 t + \boldsymbol{U}_2 t^2,\\
&\boldsymbol{V}(t) = \boldsymbol{V}_0 + \boldsymbol{V}_1 t + \boldsymbol{V}_2 t^2,\\
&\bar{\boldsymbol{u}}(t) = \bar{\boldsymbol{u}}_0 + \bar{\boldsymbol{u}}_1 t + \bar{\boldsymbol{u}}_2 t^2,\\
&\bar{\boldsymbol{v}}(t) = \bar{\boldsymbol{v}}_0 + \bar{\boldsymbol{v}}_1 t + \bar{\boldsymbol{v}}_2 t^2.
\end{aligned} \tag{14}$$

Then from Eq. (6) ($n = 2, k = 1, 2$) we get

$$(\boldsymbol{U}_1 - \boldsymbol{V}_0)\left(\frac{\Delta t}{2}+a\right) + (2\boldsymbol{U}_2 - \boldsymbol{V}_1)\left(\frac{\Delta t}{3}+\frac{a}{2}\right)\Delta t - \boldsymbol{V}_2\left(\frac{\Delta t}{4}+\frac{a}{3}\right)\Delta t^2 = \boldsymbol{0}, \tag{15}$$

$$(\boldsymbol{U}_1 - \boldsymbol{V}_0)\left(\frac{\Delta t}{3}+a\right) + (2\boldsymbol{U}_2 - \boldsymbol{V}_1)\left(\frac{\Delta t}{4}+\frac{2a}{3}\right)\Delta t - \boldsymbol{V}_2\left(\frac{\Delta t}{5}+\frac{a}{2}\right)\Delta t^2 = \boldsymbol{0}. \tag{16}$$

Solving Eqs. (15) and (16) we get

$$\boldsymbol{V}_1 = 2\boldsymbol{U}_2 + a_1\boldsymbol{U}_1 - a_1\boldsymbol{V}_0, \tag{17}$$
$$\boldsymbol{V}_2 = a_2\boldsymbol{U}_1 - a_2\boldsymbol{V}_0, \tag{18}$$

where

$$a_1 = \frac{2(60a^2+32a\Delta t+6\Delta t^2)}{\Delta t(20a^2+12a\Delta t+3\Delta t^2)},$$
$$a_2 = -\frac{10(12a^2+6a\Delta t+\Delta t^2)}{\Delta t^2(20a^2+12a\Delta t+3\Delta t^2)}. \tag{19}$$

At $n = 2$ and $k = 1, 2$, Eq. (5) reduces to the following two equations:

$$(\boldsymbol{M}\boldsymbol{V}_1 + \boldsymbol{C}\boldsymbol{V}_0 + \boldsymbol{K}\boldsymbol{U}_0)\frac{\Delta t+2a}{2} + (2\boldsymbol{M}\boldsymbol{V}_2 + \boldsymbol{C}\boldsymbol{V}_1 + \boldsymbol{K}\boldsymbol{U}_1)\frac{2\Delta t+3a}{6}\Delta t + (\boldsymbol{C}\boldsymbol{V}_2 + \boldsymbol{K}\boldsymbol{U}_2)\frac{3\Delta t+4a}{12}\Delta t^2 = \boldsymbol{R}_1, \tag{20}$$

$$(\boldsymbol{M}\boldsymbol{V}_1 + \boldsymbol{C}\boldsymbol{V}_0 + \boldsymbol{K}\boldsymbol{U}_0)\frac{2\Delta t+6a}{6} + (2\boldsymbol{M}\boldsymbol{V}_2 + \boldsymbol{C}\boldsymbol{V}_1 + \boldsymbol{K}\boldsymbol{U}_1)\frac{3\Delta t+8a}{12}\Delta t + (\boldsymbol{C}\boldsymbol{V}_2 + \boldsymbol{K}\boldsymbol{U}_2)\frac{4\Delta t+10a}{20}\Delta t^2 = \boldsymbol{R}_2. \tag{21}$$

With the insertion of Eqs. (17) and (18) into Eqs. (20) and (21), the following system can be obtained (a matrix form will be used):

$$\boldsymbol{B}\begin{Bmatrix}\boldsymbol{M}\boldsymbol{U}_1\\ \boldsymbol{M}\boldsymbol{U}_2\end{Bmatrix} + \boldsymbol{D}\begin{Bmatrix}\boldsymbol{C}\boldsymbol{U}_1\\ \boldsymbol{C}\boldsymbol{U}_2\\ \boldsymbol{K}\boldsymbol{U}_1\\ \boldsymbol{K}\boldsymbol{U}_2\end{Bmatrix} = \boldsymbol{F}\begin{Bmatrix}\boldsymbol{M}\boldsymbol{U}_0\\ \boldsymbol{M}\boldsymbol{V}_0\\ \boldsymbol{C}\boldsymbol{U}_0\\ \boldsymbol{C}\boldsymbol{V}_0\\ \boldsymbol{K}\boldsymbol{U}_0\\ \boldsymbol{K}\boldsymbol{V}_0\end{Bmatrix} + \begin{Bmatrix}\boldsymbol{R}_1\\ \boldsymbol{R}_2\end{Bmatrix}, \tag{22}$$

where

$$\boldsymbol{B} = \begin{bmatrix} b_{11}\boldsymbol{I}_2 & b_{12}\boldsymbol{I}_2\\ b_{21}\boldsymbol{I}_2 & b_{22}\boldsymbol{I}_2\end{bmatrix}, \tag{23}$$
$$\boldsymbol{D} = \begin{bmatrix} d_{11}\boldsymbol{I}_2 & d_{12}\boldsymbol{I}_2 & d_{13}\boldsymbol{I}_2 & d_{14}\boldsymbol{I}_2\\ d_{21}\boldsymbol{I}_2 & d_{22}\boldsymbol{I}_2 & d_{23}\boldsymbol{I}_2 & d_{24}\boldsymbol{I}_2\end{bmatrix},$$
$$\boldsymbol{F} = \begin{bmatrix} f_{11}\boldsymbol{I}_2 & f_{12}\boldsymbol{I}_2 & f_{13}\boldsymbol{I}_2 & f_{14}\boldsymbol{I}_2 & f_{15}\boldsymbol{I}_2 & f_{16}\boldsymbol{I}_2\\ f_{21}\boldsymbol{I}_2 & f_{22}\boldsymbol{I}_2 & f_{23}\boldsymbol{I}_2 & f_{24}\boldsymbol{I}_2 & f_{25}\boldsymbol{I}_2 & f_{26}\boldsymbol{I}_2\end{bmatrix},$$
$$\boldsymbol{I}_2 = \begin{bmatrix}\boldsymbol{I} & \boldsymbol{0}\\ \boldsymbol{0} & \boldsymbol{I}\end{bmatrix},$$
$$\boldsymbol{R}_1 = \frac{1}{\Delta t}\int_0^{\Delta t}\boldsymbol{R}(t)(t+a)\,\mathrm{d}t,$$
$$\boldsymbol{R}_2 = \frac{1}{\Delta t^2}\int_0^{\Delta t}\boldsymbol{R}(t)(t^2+2at)\,\mathrm{d}t. \tag{24}$$

Here $\boldsymbol{I}$ is the unit matrix of the order m [m is the number of nodal displacements in Eq. (2)]. The coefficients b_{ij}, d_{ij} and f_{ij} can be expressed in terms of a and Δt, and are given in the Appendix. The vectors $\boldsymbol{U}_1$ and $\boldsymbol{U}_2$ can be calculated from Eq. (22) by means of a direct solver. Then the vectors $\boldsymbol{V}_1$ and $\boldsymbol{V}_2$ can be calculated from

Eqs. (17) and (18). It is necessary to note that the dimension of system (22) is twice the dimension of the system of standard methods of the second order of accuracy.

Alternatively, system (22) can be iteratively solved using a predictor/multi-corrector algorithm. To develop such an algorithm let us modify system (22). Let us multiply both sides of equation (22) by $\boldsymbol{B}^{-1}$. Then it follows that

$$\begin{Bmatrix} \boldsymbol{M}\boldsymbol{U}_1 \\ \boldsymbol{M}\boldsymbol{U}_2 \end{Bmatrix} + \boldsymbol{B}^{-1}\boldsymbol{D}\begin{Bmatrix} \boldsymbol{C}\boldsymbol{U}_1 \\ \boldsymbol{C}\boldsymbol{U}_2 \\ \boldsymbol{K}\boldsymbol{U}_1 \\ \boldsymbol{K}\boldsymbol{U}_2 \end{Bmatrix} = \boldsymbol{B}^{-1}\boldsymbol{F}\begin{Bmatrix} \boldsymbol{M}\boldsymbol{U}_0 \\ \boldsymbol{M}\boldsymbol{V}_0 \\ \boldsymbol{C}\boldsymbol{U}_0 \\ \boldsymbol{C}\boldsymbol{V}_0 \\ \boldsymbol{K}\boldsymbol{U}_0 \\ \boldsymbol{K}\boldsymbol{V}_0 \end{Bmatrix} + \boldsymbol{B}^{-1}\begin{Bmatrix} \boldsymbol{R}_1 \\ \boldsymbol{R}_2 \end{Bmatrix}, \tag{25}$$

or

$$\boldsymbol{M}\boldsymbol{U}_1 + \bar{b}_{1m}d_{m1}\boldsymbol{C}\boldsymbol{U}_1 + \bar{b}_{1m}d_{m2}\boldsymbol{C}\boldsymbol{U}_2 + \bar{b}_{1m}d_{m3}\boldsymbol{K}\boldsymbol{U}_1 + \bar{b}_{1m}d_{m4}\boldsymbol{K}\boldsymbol{U}_2 = \bar{\boldsymbol{R}}_1, \tag{26}$$

and

$$\boldsymbol{M}\boldsymbol{U}_2 + \bar{b}_{2m}d_{m1}\boldsymbol{C}\boldsymbol{U}_1 + \bar{b}_{2m}d_{m2}\boldsymbol{C}\boldsymbol{U}_2 + \bar{b}_{2m}d_{m3}\boldsymbol{K}\boldsymbol{U}_1 + \bar{b}_{2m}d_{m4}\boldsymbol{K}\boldsymbol{U}_2 = \bar{\boldsymbol{R}}_2, \tag{27}$$

with

$$\begin{aligned}\bar{\boldsymbol{R}}_1 &= \bar{b}_{1m}f_{m1}\boldsymbol{M}\boldsymbol{U}_0 + \bar{b}_{1m}f_{m2}\boldsymbol{M}\boldsymbol{V}_0 + \bar{b}_{1m}f_{m3}\boldsymbol{C}\boldsymbol{U}_0 + \bar{b}_{1m}f_{m4}\boldsymbol{C}\boldsymbol{V}_0 \\ &\quad + \bar{b}_{1m}f_{m5}\boldsymbol{K}\boldsymbol{U}_0 + \bar{b}_{1m}f_{m6}\boldsymbol{K}\boldsymbol{V}_0 + \bar{b}_{11}\boldsymbol{R}_1 + \bar{b}_{12}\boldsymbol{R}_2, \\ \bar{\boldsymbol{R}}_2 &= \bar{b}_{2m}f_{m1}\boldsymbol{M}\boldsymbol{U}_0 + \bar{b}_{2m}f_{m2}\boldsymbol{M}\boldsymbol{V}_0 + \bar{b}_{2m}f_{m3}\boldsymbol{C}\boldsymbol{U}_0 + \bar{b}_{2m}f_{m4}\boldsymbol{C}\boldsymbol{V}_0 \\ &\quad + \bar{b}_{2m}f_{m5}\boldsymbol{K}\boldsymbol{U}_0 + \bar{b}_{2m}f_{m6}\boldsymbol{K}\boldsymbol{V}_0 + \bar{b}_{21}\boldsymbol{R}_1 + \bar{b}_{22}\boldsymbol{R}_2.\end{aligned} \tag{28}$$

In Eqs. (26)–(28) the summation over the repeated index m is meant ($m = 1, 2$), and the coefficients $\bar{b}_{ij}$ can be found as elements of the inverse matrix formed by coefficients b_{ij}; i.e.,

$$\begin{bmatrix} \bar{b}_{11} & \bar{b}_{12} \\ \bar{b}_{21} & \bar{b}_{22} \end{bmatrix} = \begin{bmatrix} b_{11} & b_{12} \\ b_{21} & b_{22} \end{bmatrix}^{-1}. \tag{29}$$

It can been checked that the matrix in Eq. (29) formed by the coefficients b_{ij} is non-singular for all values of a and Δt, and the inverse matrix always exists. Now the following recurrence relations can be suggested for the iterative solutions of Eqs. (26) and (27):

$$\begin{aligned}\bar{\boldsymbol{M}}\boldsymbol{U}_1{}^k &= \gamma_1\boldsymbol{C}\boldsymbol{U}_1{}^{k-1} + \gamma_2\boldsymbol{K}\boldsymbol{U}_1{}^{k-1} \\ &\quad - \bar{b}_{1m}d_{m1}\boldsymbol{C}\boldsymbol{U}_1{}^{k-1} - \bar{b}_{1m}d_{m2}\boldsymbol{C}\boldsymbol{U}_2{}^{k-1} \\ &\quad - \bar{b}_{1m}d_{m3}\boldsymbol{K}\boldsymbol{U}_1{}^{k-1} - \bar{b}_{1m}d_{m4}\boldsymbol{K}\boldsymbol{U}_2{}^{k-1} + \bar{\boldsymbol{R}}_1,\end{aligned} \tag{30}$$

$$\begin{aligned}\bar{\boldsymbol{M}}\boldsymbol{U}_2{}^{\bar{k}} &= \gamma_1\boldsymbol{C}\boldsymbol{U}_2{}^{k-1} + \gamma_2\boldsymbol{K}\boldsymbol{U}_2{}^{k-1} \\ &\quad - \bar{b}_{2m}d_{m1}\boldsymbol{C}\boldsymbol{U}_1{}^{k} - \bar{b}_{2m}d_{m2}\boldsymbol{C}\boldsymbol{U}_2{}^{k-1} \\ &\quad - \bar{b}_{2m}d_{m3}\boldsymbol{K}\boldsymbol{U}_1{}^{k} - \bar{b}_{2m}d_{m4}\boldsymbol{K}\boldsymbol{U}_2{}^{k-1} + \bar{\boldsymbol{R}}_2\end{aligned} \tag{31}$$

and

$$\begin{aligned}\bar{\boldsymbol{M}}\boldsymbol{U}_2{}^{k} &= \gamma_1\boldsymbol{C}\boldsymbol{U}_2{}^{\bar{k}} + \gamma_2\boldsymbol{K}\boldsymbol{U}_2{}^{\bar{k}} \\ &\quad - \bar{b}_{2m}d_{m1}\boldsymbol{C}\boldsymbol{U}_1{}^{k} - \bar{b}_{2m}d_{m2}\boldsymbol{C}\boldsymbol{U}_2{}^{\bar{k}} \\ &\quad - \bar{b}_{2m}d_{m3}\boldsymbol{K}\boldsymbol{U}_1{}^{k} - \bar{b}_{2m}d_{m4}\boldsymbol{K}\boldsymbol{U}_2{}^{\bar{k}} + \bar{\boldsymbol{R}}_2,\end{aligned} \tag{32}$$

where

$$\bar{\boldsymbol{M}} = \boldsymbol{M} + \gamma_1\boldsymbol{C} + \gamma_2\boldsymbol{K}. \tag{33}$$

Here, the parameters γ_1 and γ_2 in Eqs. (30)–(33) can be selected by means of accuracy and stability analysis of the iterative solver (see below); k is the number of the current iteration ($k = 1, 2, \ldots, l$); zero initial values are taken for $\boldsymbol{U}_1{}^0$ and $\boldsymbol{U}_2{}^0$; i.e., $\boldsymbol{U}_1{}^0 = \boldsymbol{U}_2{}^0 = \boldsymbol{0}$. It is necessary to note that for each iteration one correction for the vector $\boldsymbol{U}_1$ and two corrections for the vector $\boldsymbol{U}_2$ are used. In the case of zero damping ($\boldsymbol{C} = \boldsymbol{0}$) just one correction for the vector $\boldsymbol{U}_2$ should be used; i.e., instead of being expresses as two equations (31) and (32), the following equation should be written

$$\begin{aligned}\bar{\boldsymbol{M}}\boldsymbol{U}_2{}^{k} &= \gamma_2\boldsymbol{K}\boldsymbol{U}_2{}^{k-1} \\ &\quad - \bar{b}_{2m}d_{m3}\boldsymbol{K}\boldsymbol{U}_1{}^{k} - \bar{b}_{2m}d_{m4}\boldsymbol{K}\boldsymbol{U}_2{}^{k-1} + \bar{\boldsymbol{R}}_2.\end{aligned} \tag{34}$$

The accuracy analysis (see below) shows that only two iterations ($k = 1, 2$) are necessary in order to reach the same order of accuracy that a direct solver yields; i.e., when Eqs. (22) are solved simultaneously.

Remark For zero and non-zero damping matrices $\boldsymbol{C}$, different iterative predictor/multi-corrector solvers are used for the solution of elastodynamics problems; i.e., Eq. (34) does not follow from Eqs. (31) and (32).

2.4 Third-order time approximations ($n = 3$)

For the third-order approximations of the vectors $\boldsymbol{U}(t)$, $\boldsymbol{V}(t), \bar{\boldsymbol{u}}(t)$ and $\bar{\boldsymbol{v}}(t)$, Eq. (4) can be rewritten as follows

$$\begin{aligned}
\boldsymbol{U}(t) &= \boldsymbol{U}_0 + \boldsymbol{U}_1 t + \boldsymbol{U}_2 t^2 + \boldsymbol{U}_3 t^3,\\
\boldsymbol{V}(t) &= \boldsymbol{V}_0 + \boldsymbol{V}_1 t + \boldsymbol{V}_2 t^2 + \boldsymbol{V}_3 t^3,\\
\bar{\boldsymbol{u}}(t) &= \bar{\boldsymbol{u}}_0 + \bar{\boldsymbol{u}}_1 t + \bar{\boldsymbol{u}}_2 t^2 + \bar{\boldsymbol{u}}_3 t^3,\\
\bar{\boldsymbol{v}}(t) &= \bar{\boldsymbol{v}}_0 + \bar{\boldsymbol{v}}_1 t + \bar{\boldsymbol{v}}_2 t^2 + \bar{\boldsymbol{v}}_3 t^3.
\end{aligned} \tag{35}$$

Then from Eq. (6) ($n = 3, k = 1, 2, 3$), we get

$$\begin{aligned}
&(\boldsymbol{U}_1 - \boldsymbol{V}_0)\left(\frac{\Delta t}{2} + a\right) + (2\boldsymbol{U}_2 - \boldsymbol{V}_1)\left(\frac{\Delta t}{3} + \frac{a}{2}\right)\Delta t\\
&\quad + (3\boldsymbol{U}_3 - \boldsymbol{V}_2)\left(\frac{\Delta t}{4} + \frac{a}{3}\right)\Delta t^2\\
&\quad - \boldsymbol{V}_3\left(\frac{\Delta t}{5} + \frac{a}{4}\right)\Delta t^3 = \boldsymbol{0}, \qquad (36)\\
&(\boldsymbol{U}_1 - \boldsymbol{V}_0)\left(\frac{\Delta t}{3} + a\right) + (2\boldsymbol{U}_2 - \boldsymbol{V}_1)\left(\frac{\Delta t}{4} + \frac{2a}{3}\right)\Delta t\\
&\quad + (3\boldsymbol{U}_3 - \boldsymbol{V}_2)\left(\frac{\Delta t}{5} + \frac{a}{2}\right)\Delta t^2\\
&\quad - \boldsymbol{V}_3\left(\frac{\Delta t}{6} + \frac{2a}{5}\right)\Delta t^3 = \boldsymbol{0}, \qquad (37)\\
&(\boldsymbol{U}_1 - \boldsymbol{V}_0)\left(\frac{\Delta t}{4} + a\right) + (2\boldsymbol{U}_2 - \boldsymbol{V}_1)\left(\frac{\Delta t}{5} + \frac{3a}{4}\right)\Delta t\\
&\quad + (3\boldsymbol{U}_3 - \boldsymbol{V}_2)\left(\frac{\Delta t}{6} + \frac{3a}{5}\right)\Delta t^2\\
&\quad - \boldsymbol{V}_3\left(\frac{\Delta t}{7} + \frac{a}{2}\right)\Delta t^3 = \boldsymbol{0}. \qquad (38)
\end{aligned}$$

Solving Eqs. (36)–(38), we get

$$\boldsymbol{V}_1 = 2\boldsymbol{U}_2 + a_1\boldsymbol{U}_1 - a_1\boldsymbol{V}_0, \tag{39}$$
$$\boldsymbol{V}_2 = 3\boldsymbol{U}_3 + a_2\boldsymbol{U}_1 - a_2\boldsymbol{V}_0, \tag{40}$$
$$\boldsymbol{V}_3 = a_3\boldsymbol{U}_1 - a_3\boldsymbol{V}_0, \tag{41}$$

where

$$\begin{aligned}
a_1 &= \frac{15(84a^3 + 45a^2\Delta t + 10a\Delta t^2 + \Delta t^3)}{\Delta t(105a^3 + 60a^2\Delta t + 15a\Delta t^2 + 2\Delta t^3)},\\
a_2 &= -\frac{15(420a^3 + 216a^2\Delta t + 45a\Delta t^2 + 4\Delta t^3)}{2\Delta t^2(105a^3 + 60a^2\Delta t + 15a\Delta t^2 + 2\Delta t^3)},\\
a_3 &= \frac{35(120a^3 + 60a^2\Delta t + 12a\Delta t^2 + 4\Delta t^3)}{2\Delta t^3(105a^3 + 60a^2\Delta t + 15a\Delta t^2 + 2\Delta t^3)}.
\end{aligned} \tag{42}$$

At $n = 3$ and $k = 1, 2, 3$, Eq. (5) reduces to the following three equations:

$$\begin{aligned}
&(\boldsymbol{M}\boldsymbol{V}_1 + \boldsymbol{C}\boldsymbol{V}_0 + \boldsymbol{K}\boldsymbol{U}_0)\frac{\Delta t + 2a}{2}\\
&\quad + (2\boldsymbol{M}\boldsymbol{V}_2 + \boldsymbol{C}\boldsymbol{V}_1 + \boldsymbol{K}\boldsymbol{U}_1)\frac{2\Delta t + 3a}{6}\Delta t\\
&\quad + (3\boldsymbol{M}\boldsymbol{V}_3 + \boldsymbol{C}\boldsymbol{V}_2 + \boldsymbol{K}\boldsymbol{U}_2)\frac{3\Delta t + 4a}{12}\Delta t^2\\
&\quad + (\boldsymbol{C}\boldsymbol{V}_3 + \boldsymbol{K}\boldsymbol{U}_3)\frac{4\Delta t + 5a}{20}\Delta t^3 = \boldsymbol{R}_1, \qquad (43)\\
&(\boldsymbol{M}\boldsymbol{V}_1 + \boldsymbol{C}\boldsymbol{V}_0 + \boldsymbol{K}\boldsymbol{U}_0)\frac{2\Delta t + 6a}{6}\\
&\quad + (2\boldsymbol{M}\boldsymbol{V}_2 + \boldsymbol{C}\boldsymbol{V}_1 + \boldsymbol{K}\boldsymbol{U}_1)\frac{3\Delta t + 8a}{12}\Delta t\\
&\quad + (3\boldsymbol{M}\boldsymbol{V}_3 + \boldsymbol{C}\boldsymbol{V}_2 + \boldsymbol{K}\boldsymbol{U}_2)\frac{4\Delta t + 10a}{20}\Delta t^2\\
&\quad + (\boldsymbol{C}\boldsymbol{V}_3 + \boldsymbol{K}\boldsymbol{U}_3)\frac{5\Delta t + 12a}{30}\Delta t^3 = \boldsymbol{R}_2, \qquad (44)\\
&(\boldsymbol{M}\boldsymbol{V}_1 + \boldsymbol{C}\boldsymbol{V}_0 + \boldsymbol{K}\boldsymbol{U}_0)\frac{3\Delta t + 12a}{12}\\
&\quad + (2\boldsymbol{M}\boldsymbol{V}_2 + \boldsymbol{C}\boldsymbol{V}_1 + \boldsymbol{K}\boldsymbol{U}_1)\frac{4\Delta t + 15a}{20}\Delta t\\
&\quad + (3\boldsymbol{M}\boldsymbol{V}_3 + \boldsymbol{C}\boldsymbol{V}_2 + \boldsymbol{K}\boldsymbol{U}_2)\frac{5\Delta t + 18a}{30}\Delta t^2\\
&\quad + (\boldsymbol{C}\boldsymbol{V}_3 + \boldsymbol{K}\boldsymbol{U}_3)\frac{6\Delta t + 21a}{42}\Delta t^3 = \boldsymbol{R}_3. \qquad (45)
\end{aligned}$$

By the insertion of Eqs. (39)–(41) into Eqs. (43)–(45), the following system can be obtained (a matrix form will be used):

$$\boldsymbol{B}\begin{Bmatrix}\boldsymbol{M}\boldsymbol{U}_1\\ \boldsymbol{M}\boldsymbol{U}_2\\ \boldsymbol{M}\boldsymbol{U}_3\end{Bmatrix} + \boldsymbol{D}\begin{Bmatrix}\boldsymbol{C}\boldsymbol{U}_1\\ \boldsymbol{C}\boldsymbol{U}_2\\ \boldsymbol{C}\boldsymbol{U}_3\\ \boldsymbol{K}\boldsymbol{U}_1\\ \boldsymbol{K}\boldsymbol{U}_2\\ \boldsymbol{K}\boldsymbol{U}_3\end{Bmatrix} = \boldsymbol{F}\begin{Bmatrix}\boldsymbol{M}\boldsymbol{U}_0\\ \boldsymbol{M}\boldsymbol{V}_0\\ \boldsymbol{C}\boldsymbol{U}_0\\ \boldsymbol{C}\boldsymbol{V}_0\\ \boldsymbol{K}\boldsymbol{U}_0\\ \boldsymbol{K}\boldsymbol{V}_0\end{Bmatrix} + \begin{Bmatrix}\boldsymbol{R}_1\\ \boldsymbol{R}_2\\ \boldsymbol{R}_3\end{Bmatrix}, \tag{46}$$

where

$$\boldsymbol{B} = \begin{bmatrix} b_{11}\boldsymbol{I}_3 & b_{12}\boldsymbol{I}_3 & b_{13}\boldsymbol{I}_3\\ b_{21}\boldsymbol{I}_3 & b_{22}\boldsymbol{I}_3 & b_{23}\boldsymbol{I}_3\\ b_{31}\boldsymbol{I}_3 & b_{32}\boldsymbol{I}_3 & b_{33}\boldsymbol{I}_3\end{bmatrix}, \tag{47}$$

$$\boldsymbol{D} = \begin{bmatrix} d_{11}\boldsymbol{I}_3 & d_{12}\boldsymbol{I}_3 & d_{13}\boldsymbol{I}_3 & d_{14}\boldsymbol{I}_3 & d_{15}\boldsymbol{I}_3 & d_{16}\boldsymbol{I}_3\\ d_{21}\boldsymbol{I}_3 & d_{22}\boldsymbol{I}_3 & d_{23}\boldsymbol{I}_3 & d_{24}\boldsymbol{I}_3 & d_{25}\boldsymbol{I}_3 & d_{26}\boldsymbol{I}_3\\ d_{31}\boldsymbol{I}_3 & d_{32}\boldsymbol{I}_3 & d_{33}\boldsymbol{I}_3 & d_{34}\boldsymbol{I}_3 & d_{35}\boldsymbol{I}_3 & d_{36}\boldsymbol{I}_3\end{bmatrix},$$

$$\boldsymbol{F} = \begin{bmatrix} f_{11}\boldsymbol{I}_3 & f_{12}\boldsymbol{I}_3 & f_{13}\boldsymbol{I}_3 & f_{14}\boldsymbol{I}_3 & f_{15}\boldsymbol{I}_3 & f_{16}\boldsymbol{I}_3 \\ f_{21}\boldsymbol{I}_3 & f_{22}\boldsymbol{I}_3 & f_{23}\boldsymbol{I}_3 & f_{24}\boldsymbol{I}_3 & f_{25}\boldsymbol{I}_3 & f_{26}\boldsymbol{I}_3 \\ f_{31}\boldsymbol{I}_3 & f_{32}\boldsymbol{I}_3 & f_{33}\boldsymbol{I}_3 & f_{34}\boldsymbol{I}_3 & f_{35}\boldsymbol{I}_3 & f_{36}\boldsymbol{I}_3 \end{bmatrix},$$

$$\boldsymbol{I}_3 = \begin{bmatrix} \boldsymbol{I}\,\boldsymbol{0}\,\boldsymbol{0} \\ \boldsymbol{0}\,\boldsymbol{I}\,\boldsymbol{0} \\ \boldsymbol{0}\,\boldsymbol{0}\,\boldsymbol{I} \end{bmatrix},$$

$$\boldsymbol{R}_1 = \frac{1}{\Delta t}\int_0^{\Delta t} \boldsymbol{R}(t)(t + a)\,\mathrm{d}t,$$

$$\boldsymbol{R}_2 = \frac{1}{\Delta t^2}\int_0^{\Delta t} \boldsymbol{R}(t)(t^2 + 2at)\,\mathrm{d}t, \tag{48}$$

$$\boldsymbol{R}_3 = \frac{1}{\Delta t^3}\int_0^{\Delta t} \boldsymbol{R}(t)(t^3 + 3at^2)\,\mathrm{d}t.$$

The coefficients b_{ij}, d_{ij} and f_{ij} can be expressed in terms of a and Δt, and are given in the Appendix. The vectors $\boldsymbol{U}_1, \boldsymbol{U}_2$, and $\boldsymbol{U}_3$ can be calculated from Eq. (46) by means of a direct solver. Then the vectors $\boldsymbol{V}_1$, $\boldsymbol{V}_2$ and $\boldsymbol{V}_3$ can be calculated from Eqs. (39)–(41). It is necessary to note that the dimension of system (46) is three times as large as the dimension of the system of standard methods of the second order of accuracy.

Alternatively, system (46) can be iteratively solved by means of a predictor/multi-corrector algorithm similarly as it was solved with quadratic time approximations ($n = 2$). Let us multiply both sides of equation (46) by $\boldsymbol{B}^{-1}$. Then it follows that

$$\begin{Bmatrix} \boldsymbol{M}\boldsymbol{U}_1 \\ \boldsymbol{M}\boldsymbol{U}_2 \\ \boldsymbol{M}\boldsymbol{U}_3 \end{Bmatrix} + \boldsymbol{B}^{-1}\boldsymbol{D}\begin{Bmatrix} \boldsymbol{C}\boldsymbol{U}_1 \\ \boldsymbol{C}\boldsymbol{U}_2 \\ \boldsymbol{C}\boldsymbol{U}_3 \\ \boldsymbol{K}\boldsymbol{U}_1 \\ \boldsymbol{K}\boldsymbol{U}_2 \\ \boldsymbol{K}\boldsymbol{U}_3 \end{Bmatrix} = \boldsymbol{B}^{-1}\boldsymbol{F}\begin{Bmatrix} \boldsymbol{M}\boldsymbol{U}_0 \\ \boldsymbol{M}\boldsymbol{V}_0 \\ \boldsymbol{C}\boldsymbol{U}_0 \\ \boldsymbol{C}\boldsymbol{V}_0 \\ \boldsymbol{K}\boldsymbol{U}_0 \\ \boldsymbol{K}\boldsymbol{V}_0 \end{Bmatrix} + \boldsymbol{B}^{-1}\begin{Bmatrix} \boldsymbol{R}_1 \\ \boldsymbol{R}_2 \\ \boldsymbol{R}_3 \end{Bmatrix}, \tag{49}$$

or

$$\boldsymbol{M}\boldsymbol{U}_i + \bar{b}_{im}d_{mp}\boldsymbol{C}\boldsymbol{U}_p + \bar{b}_{im}d_{m(p+3)}\boldsymbol{K}\boldsymbol{U}_p = \bar{\boldsymbol{R}}_i, \qquad i = 1,2,3 \tag{50}$$

with

$$\bar{\boldsymbol{R}}_i = \bar{b}_{im}f_{m1}\boldsymbol{M}\boldsymbol{U}_0 + \bar{b}_{im}f_{m2}\boldsymbol{M}\boldsymbol{V}_0 + \bar{b}_{im}f_{m3}\boldsymbol{C}\boldsymbol{U}_0 + \bar{b}_{im}f_{m4}\boldsymbol{C}\boldsymbol{V}_0 + \bar{b}_{im}f_{m5}\boldsymbol{K}\boldsymbol{U}_0 + \bar{b}_{im}f_{m6}\boldsymbol{K}\boldsymbol{V}_0 + \bar{b}_{im}\boldsymbol{R}_m, \quad i = 1,2,3. \tag{51}$$

In Eqs. (50), (51) the summation over the repeated indices m and p is meant ($m = 1,2,3$ and $p = 1,2,3$), and the coefficients $\bar{b}_{ij}$ can be found as elements of the inverse matrix formed by coefficients b_{ij}; i.e.,

$$\begin{bmatrix} \bar{b}_{11} & \bar{b}_{12} & \bar{b}_{13} \\ \bar{b}_{21} & \bar{b}_{22} & \bar{b}_{23} \\ \bar{b}_{31} & \bar{b}_{32} & \bar{b}_{33} \end{bmatrix} = \begin{bmatrix} b_{11} & b_{12} & b_{13} \\ b_{21} & b_{22} & b_{23} \\ b_{31} & b_{32} & b_{33} \end{bmatrix}^{-1}. \tag{52}$$

Remark For the third-order time approximations the matrix in Eq. (52) formed by the coefficients b_{ij} is singular if the following condition is met

$$120a^3 + 60a^2\Delta t + 12a\Delta t^2 + \Delta t^3 = 0. \tag{53}$$

That is, at a given Δt, the values of a that satisfy (53) must be avoided for the calculation of the inverse matrix.

Now the following recurrence relations can be suggested for the iterative solutions of Eq. (50)

$$\begin{aligned} \bar{\boldsymbol{M}}\boldsymbol{U}_1{}^k = {} & \gamma_1\boldsymbol{C}\boldsymbol{U}_1{}^{k-1} + \gamma_2\boldsymbol{K}\boldsymbol{U}_1{}^{k-1} \\ & - \bar{b}_{1m}d_{m1}\boldsymbol{C}\boldsymbol{U}_1{}^{k-1} - \bar{b}_{1m}d_{m2}\boldsymbol{C}\boldsymbol{U}_2{}^{k-1} \\ & - \bar{b}_{1m}d_{m3}\boldsymbol{C}\boldsymbol{U}_3{}^{k-1} - \bar{b}_{1m}d_{m4}\boldsymbol{K}\boldsymbol{U}_1{}^{k-1} \\ & - \bar{b}_{1m}d_{m5}\boldsymbol{K}\boldsymbol{U}_2{}^{k-1} - \bar{b}_{1m}d_{m6}\boldsymbol{K}\boldsymbol{U}_3{}^{k-1} + \bar{\boldsymbol{R}}_1, \end{aligned} \tag{54}$$

$$\begin{aligned} \bar{\boldsymbol{M}}\boldsymbol{U}_2{}^k = {} & \gamma_1\boldsymbol{C}\boldsymbol{U}_2{}^{k-1} + \gamma_2\boldsymbol{K}\boldsymbol{U}_2{}^{k-1} \\ & - \bar{b}_{2m}d_{m1}\boldsymbol{C}\boldsymbol{U}_1{}^{k} - \bar{b}_{2m}d_{m2}\boldsymbol{C}\boldsymbol{U}_2{}^{k-1} \\ & - \bar{b}_{2m}d_{m3}\boldsymbol{C}\boldsymbol{U}_3{}^{k-1} - \bar{b}_{2m}d_{m4}\boldsymbol{K}\boldsymbol{U}_1{}^{k} \\ & - \bar{b}_{2m}d_{m5}\boldsymbol{K}\boldsymbol{U}_2{}^{k-1} - \bar{b}_{2m}d_{m6}\boldsymbol{K}\boldsymbol{U}_3{}^{k-1} + \bar{\boldsymbol{R}}_2, \end{aligned} \tag{55}$$

and

$$\begin{aligned} \bar{\boldsymbol{M}}\boldsymbol{U}_3{}^{\bar{k}} = {} & \gamma_1\boldsymbol{C}\boldsymbol{U}_3{}^{k-1} + \gamma_2\boldsymbol{K}\boldsymbol{U}_3{}^{k-1} \\ & - \bar{b}_{3m}d_{m1}\boldsymbol{C}\boldsymbol{U}_1{}^{k} - \bar{b}_{3m}d_{m2}\boldsymbol{C}\boldsymbol{U}_2{}^{k} \\ & - \bar{b}_{3m}d_{m3}\boldsymbol{C}\boldsymbol{U}_3{}^{k-1} - \bar{b}_{3m}d_{m4}\boldsymbol{K}\boldsymbol{U}_1{}^{k} \\ & - \bar{b}_{3m}d_{m5}\boldsymbol{K}\boldsymbol{U}_2{}^{k} - \bar{b}_{3m}d_{m6}\boldsymbol{K}\boldsymbol{U}_3{}^{k-1} + \bar{\boldsymbol{R}}_3, \end{aligned} \tag{56}$$

$$\begin{aligned} \bar{\boldsymbol{M}}\boldsymbol{U}_3{}^{k} = {} & \gamma_1\boldsymbol{C}\boldsymbol{U}_3{}^{\bar{k}} + \gamma_2\boldsymbol{K}\boldsymbol{U}_3{}^{\bar{k}} \\ & - \bar{b}_{3m}d_{m1}\boldsymbol{C}\boldsymbol{U}_1{}^{k} - \bar{b}_{3m}d_{m2}\boldsymbol{C}\boldsymbol{U}_2{}^{k} \\ & - \bar{b}_{3m}d_{m3}\boldsymbol{C}\boldsymbol{U}_3{}^{\bar{k}} - \bar{b}_{3m}d_{m4}\boldsymbol{K}\boldsymbol{U}_1{}^{k} \\ & - \bar{b}_{3m}d_{m5}\boldsymbol{K}\boldsymbol{U}_2{}^{k} - \bar{b}_{3m}d_{m6}\boldsymbol{K}\boldsymbol{U}_3{}^{\bar{k}} + \bar{\boldsymbol{R}}_3, \end{aligned} \tag{57}$$

where

$$\bar{\boldsymbol{M}} = \boldsymbol{M} + \gamma_1\boldsymbol{C} + \gamma_2\boldsymbol{K}. \tag{58}$$

Here, the parameters γ_1 and γ_2 in Eqs. (54)–(58) can be selected by means of accuracy and stability analysis of the iterative solver (see below); k is the number of the current iteration ($k = 1,2,\ldots,l$); zero initial values are taken for $\boldsymbol{U}_1{}^0, \boldsymbol{U}_2{}^0$ and $\boldsymbol{U}_3{}^0$; i.e., $\boldsymbol{U}_1{}^0 = \boldsymbol{U}_2{}^0 = \boldsymbol{U}_3{}^0 = \boldsymbol{0}$. It is necessary to note that for each iteration one correction for the vectors $\boldsymbol{U}_1$ and $\boldsymbol{U}_2$, and two corrections

for the vector $\boldsymbol{U}_3$ are used. In the case of zero damping ($\boldsymbol{C} = \boldsymbol{0}$) just one correction for the $\boldsymbol{U}_3$ should be used; i.e., instead of being expressed as two equations (56) and (57), the following equation should be written

$$\bar{\boldsymbol{M}}\,\boldsymbol{U}_3{}^k = \gamma_2 \boldsymbol{K}\,\boldsymbol{U}_3{}^{k-1} - \bar{b}_{3m} d_{m4} \boldsymbol{K}\,\boldsymbol{U}_1{}^k - \bar{b}_{3m} d_{m5} \boldsymbol{K}\,\boldsymbol{U}_2{}^k - \bar{b}_{3m} d_{m6} \boldsymbol{K}\,\boldsymbol{U}_3{}^{k-1} + \bar{\boldsymbol{R}}_3. \tag{59}$$

The accuracy analysis (see below) shows that only three iterations ($k = 1,2,3$) are necessary in order to reach the same order of accuracy that a direct solver yields; i.e., when Eqs. (50) are solved simultaneously.

2.5 Accuracy analysis

It can be shown (e.g., see [3,10]; A. V. Idesman, submitted) that the analysis of a numerical method for linear dynamics problems Eqs. (1) can be replaced (with the modal decomposition method) by the analysis of the method applied to a system with a single degree of freedom $u(t)$; i.e., the solution of the exact following simple equations is considered

$$\dot{v}(t) + 2\xi\, v(t) + \omega^2 u(t) = f(t), \tag{60}$$

$$\dot{u}(t) - v(t) = 0, \tag{61}$$

where ω and f are the natural frequency and forcing excitation, respectively, $v(t)$ is the velocity, ξ is the damping ratio. For the analysis of accuracy and stability of numerical methods, the interval J_n from 0 to Δt is considered.

The values of u_n and v_n at time $t = t_n$ can be expressed in terms of initial values u_0 and v_0 in the beginning of the interval J_n as

$$\left\{ \begin{matrix} u_n \\ v_n \end{matrix} \right\} = [A] \left\{ \begin{matrix} u_0 \\ v_0 \end{matrix} \right\} + [L] f, \tag{62}$$

where $[A]$ is the amplification matrix, $[L]$ is the load matrix. Without loss of generality we can assume that $t_{n-1} = 0$ and $t_n - t_{n-1} = \Delta t$.

The analytical expression of the matrix $[A]$ in Eq. (62) for direct and predictor/multi-corrector solvers can be calculated from the application of the corresponding method to the system with a single degree of freedom, Eqs. (60)–(61), at the condition $f(t) = 0$. The expansion of the analytical expressions of the elements of the exact matrix $[A]$ into the Taylor series is given below:

$$A_{11} = 1 - \frac{\omega^2\Delta t^2}{2} + \frac{\xi\omega^3\Delta t^3}{3} + \frac{(1-4\xi^2)\omega^4\Delta t^4}{24} + \frac{\xi(-1+2\xi^2)\omega^5\Delta t^5}{30} - \frac{(1-12\xi^2+16\xi^4)\omega^6\Delta t^6}{720} + \frac{\xi(3-16\xi^2+16\xi^4)\omega^7\Delta t^7}{2520} + \frac{(1-24\xi^2+80\xi^4-64\xi^6)\omega^8\Delta t^8}{40320} + O[\Delta t]^9, \tag{63}$$

$$A_{22} = 1 - 2\xi\omega\Delta t + \frac{(-1+4\xi^2)\omega^2\Delta t^2}{2} + \frac{2\xi(1-2\xi^2)\omega^3\Delta t^3}{3} + \frac{(1-12\xi^2+16\xi^4)\omega^4\Delta t^4}{24} - \frac{\xi(3-16\xi^2+16\xi^4)\omega^5\Delta t^5}{60} - \frac{(1-24\xi^2+80\xi^4-64\xi^6)\omega^6\Delta t^6}{720} + \frac{\xi(1-10\xi^2+24\xi^4-16\xi^6)\omega^7\Delta t^7}{630} + \frac{(1-40\xi^2+240\xi^4-448\xi^6+256\xi^8)\omega^8\Delta t^8}{40320} + O[\Delta t]^9, \tag{64}$$

$$A_{12} = -A_{21}/\omega^2 = \Delta t - \xi\omega\Delta t^2 + \frac{(-1+4\xi^2)\omega^2\Delta t^3}{6} - \frac{\xi(-1+2\xi^2)\omega^3\Delta t^4}{6} + \frac{(1-12\xi^2+16\xi^4)\omega^4\Delta t^5}{120} - \frac{\xi(3-16\xi^2+16\xi^4)\omega^5\Delta t^6}{360} - \frac{(1-24\xi^2+80\xi^4-64\xi^6)\omega^6\Delta t^7}{5040} + \frac{\xi(1-10\xi^2+24\xi^4-16\xi^6)\omega^7\Delta t^8}{5040} + O[\Delta t]^9. \tag{65}$$

The accuracy of the new TCG method can be estimated by the application of this method to system (60)-(61) and by the comparison of the numerical and exact (Eqs. (63)–(65)) amplification matrices (see [10]; A.V. Idesman, submitted).

The stability of an algorithm can be observed from the spectral radius defined by $r(\boldsymbol{A}) = \max|\rho_1, \rho_2|$, where ρ_1 and ρ_2 denote the eigenvalues of the amplification matrix $[A]$ (see [10]). An algorithm that satisfies the condition $r(\boldsymbol{A}) \le 1$ is said to be unconditionally stable. It is known that the higher modes of semidiscrete structural equations do not represent the behavior of the governing partial differential equations. Therefore, some form of algorithmic damping (dissipation) is necessary in order to remove the participation of the high-frequency modal components. The numerical dissipation of the algorithm over the entire frequency domain can be observed from the spectral radius. The condition $r(\boldsymbol{A})$=1 for some frequencies corresponds to non-dissipative

behavior, and $r(\boldsymbol{A}) < 1$ for some frequencies corresponds to the introduction of the numerical dissipation. It is desirable to design a numerical algorithm with non-dissipative properties at low frequencies and with large numerical dissipation at high frequencies.

2.6 Linear time approximations ($n = 1$)

Let us consider the numerical amplification matrix $[A]$. The highest-order terms in the expansion of the elements of the matrix $[A]$ into the Taylor series, which differ from Eqs. (63)–(65), are given below:

$$A_{11} = \cdots + \frac{\omega^2(-1 + 6a\xi\omega)\Delta t^3}{12a} + O[\Delta t]^4, \tag{66}$$

$$A_{22} = \cdots + \frac{\omega^2(-1 + 4\xi^2 + 12a\xi\omega - 24a\xi^3\omega)\Delta t^3}{12a} + O[\Delta t]^4, \tag{67}$$

$$A_{12} = -A_{21}/\omega^2 = \cdots + \frac{\omega(-2\xi + 3(-1 + 4\xi^2)a\omega)\Delta t^3}{12a} + O[\Delta t]^4. \tag{68}$$

The spectral radius of the numerical amplification matrix $[A]$, which depends on $\omega, \Delta t, a$ and ξ, can be represented as a function of the three parameters $\Omega = \omega\Delta t, \alpha = \Delta t/a$ and ξ; i.e., $r = r(\Omega, \alpha, \xi)$. The spectral radii of the numerical matrix $[A]$ are given in Fig. 1.

2.7 Quadratic time approximations ($n = 2$)

Let us separately consider the TCG method with a direct solver and the suggested predictor/multi-corrector solver without damping and with damping.

2.7.1 A direct solver

The highest-order terms in the expansion of the elements of the matrix $[A]$ into the Taylor series, which differ from Eqs. (63)–(65), are given below:

$$A_{11} = \cdots + [\omega^3(-a\omega + 4a\xi^2\omega + 40a^2\xi^3\omega^2 - 2\xi(1 + 10a^2\omega^2))\Delta t^5]/720a^2 + O[\Delta t]^6, \tag{69}$$

$$A_{22} = \cdots - [\omega^3(a\omega - 12a\xi^2\omega + 16a\xi^4\omega + 160a^2\xi^5\omega^2 - 8\xi^3(1 + 20a^2\omega^2) + \xi(4 + 30a^2\omega^2))\Delta t^5]/720a^2 + O[\Delta t]^6, \tag{70}$$

$$A_{12} = -A_{21}/\omega^2 = \cdots + [\omega^2(1 - 4a\xi\omega + 8a\xi^3\omega + 5a^2\omega^2 + 80a^2\xi^4\omega^2 - 4\xi^2(1 + 15a^2\omega^2))\Delta t^5]/720a^2 + O[\Delta t]^6. \tag{71}$$

The spectral radii $r = r(\Omega, \alpha, \xi)$ of the numerical matrix $[A]$ are given in Fig. 2.

2.7.2 The predictor/multi-corrector solver (without damping)

We will analyze the amplification matrix $[A]$ after two iterations with only one correction of the vector $\boldsymbol{U}_2$ (see Eqs. (30) and (34)). The following representations of the parameters $\gamma_1 = 0$ and $\gamma_2 = \gamma_3\Delta t^2$ in Eq. (33) are used for the analysis (γ_3 is a new parameter). The highest-order terms in the expansion of the elements of the matrix $[A]$ into the Taylor series, which differ from Eqs. (63)–(65), are given below:

$$A_{11} = \cdots - \frac{\omega^4\Delta t^5}{720a} + O[\Delta t]^6, \tag{72}$$

$$A_{22} = \cdots - \frac{((1 + 12\gamma_3 + 72\gamma_3^2)\omega^4)\Delta t^5}{360a} + O[\Delta t]^6, \tag{73}$$

$$A_{12} = \cdots + \frac{(\omega^2 - 120a^2\gamma_3(1 + 6\gamma_3)\omega^4)\Delta t^5}{720a^2} + O[\Delta t]^6, \tag{74}$$

$$A_{21} = \cdots + \frac{\omega^4(-1 + 15a^2(1 - 16\gamma_3 + 48\gamma_3^2)\omega^2)\Delta t^5}{720a^2} + O[\Delta t]^6. \tag{75}$$

For the predictor/multi-corrector solver the spectral radius is a function of $\omega, \Delta t, a$ and ξ and can not be simplified as for a direct solver. The spectral radii of the numerical matrix $[A]$ are given in Fig. 3.

2.7.3 The predictor/multi-corrector solver (with damping)

We will analyze the amplification matrix $[A]$ after two iterations (see Eqs. (30)–(32)). The following representations of the parameters $\gamma_1 = 0$ and $\gamma_2 = \gamma_3\Delta t^2$ in Eq. (33) are used for the analysis (γ_3 is a new parameter).The

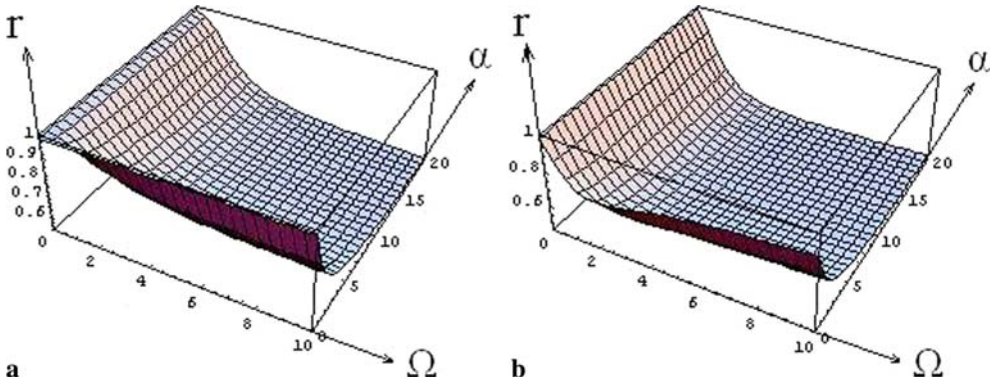

Fig. 1 Spectral radii r for the TCG method with linear approximations in time for $\xi = 0$ (**a**) and $\xi = 0.3$ (**b**)

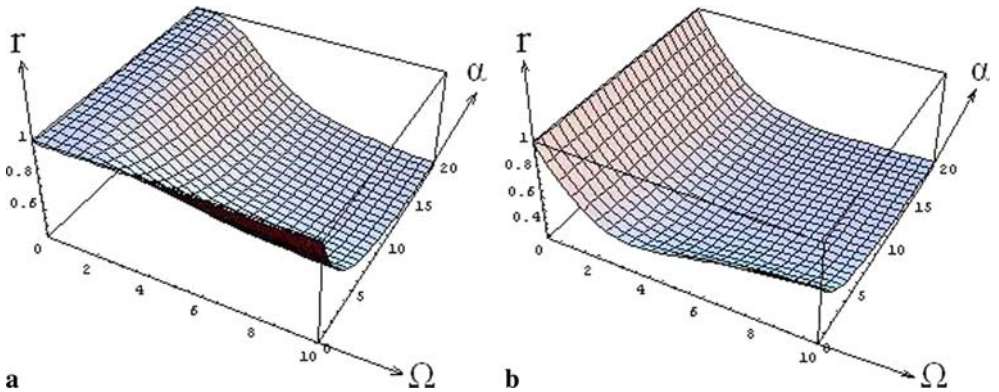

Fig. 2 Spectral radii r for the TCG method with quadratic approximations in time and a direct solver for $\xi = 0$ (**a**) and $\xi = 0.3$ (**b**)

highest-order terms in the expansion of the elements of the matrix $[A]$ into the Taylor series, which differ from Eqs. (63)–(65), are given below:

$$A_{11} = \cdots + [\omega^3(-a\omega + 4a\xi^2\omega + 120a^2\xi^3\omega^2 + 2\xi(-1 + 5a^2(-1 + 12\gamma_3)\omega^2)\Delta t^5]/720a^2 + O[\Delta t]^6, \quad (76)$$

$$A_{22} = \cdots + \omega^3(-a(1 + 12\gamma_3 + 72\gamma_3^2)\omega + 2a(5 + 24\gamma_3)\xi^2\omega + 8a\xi^4\omega + 240a^2\xi^5\omega^2 + 4\xi^3(1 + 5a^2(5 + 12\gamma_3)\omega^2) + 2\xi(-1 + 5a^2(-1 + 12\gamma_3 + 72\gamma_3^2)\omega^2))\Delta t^5]/360a^2 + O[\Delta t]^6, \quad (77)$$

$$A_{12} = \cdots + [\omega^2(1 - 4a\xi\omega + 8a\xi^3\omega - 120a^2\gamma_3(1 + 6\gamma_3)\omega^2 + 240a^2\xi^4\omega^2 + 4\xi^2(-1 + 5a^2(-1 + 24\gamma_3)\omega^2))\Delta t^5]/720a^2 + O[\Delta t]^6, \quad (78)$$

$$A_{21} = \cdots + [\omega^4(-1 + 6a(1 + 4\gamma_3)\xi\omega + 8a\xi^3\omega - 5a^2\omega^2 + 240a^2\xi^4\omega^2 + \xi^2(4 - 40a^2(-1 + 6\gamma_3)\omega^2))\Delta t^5]/720a^2 + O[\Delta t]^6. \quad (79)$$

Because the eigenvalues of the numerical amplification matrix $[A]$ are not always complex conjugate, we will present absolute values of two eigenvectors ρ_1 and ρ_2 (see Fig. 3).

2.8 Third-order time approximations ($n = 3$)

Let us separately consider the TCG method with a direct solver and the suggested predictor/multi-corrector solver without damping and with damping.

2.8.1 A direct solver

The highest-order terms in the expansion of the elements of the matrix $[A]$ into the Taylor series, which differ from Eqs. (63)–(65), are given below:

$$A_{11} = \cdots + [\omega^4(1 - a^2\omega^2 - 16a^2\xi^4\omega^2 + 672a^3\xi^5\omega^3 + 4\xi^2(-1 + 3a^2\omega^2) + 2a\xi\omega(-2 + 63a^2\omega^2) + \xi^3(8a\omega - 672a^3\omega^3))\Delta t^7]/100800a^3 + O[\Delta t]^8, \quad (80)$$

$$A_{22} = \cdots + [\omega^4(1 - a^2\omega^2 + 64a^2\xi^6\omega^2 - 2688a^3\xi^7\omega^3 + \xi^4(16 - 80a^2\omega^2) + 12\xi^2(-1 + 2a^2\omega^2) + 6a\xi\omega(-1 + 28a^2\omega^2) + 32a\xi^5\omega(-1 + 126a^2\omega^2) + \xi^3(32a\omega - 1680a^3\omega^3))\Delta t^7]/100800a^3 + O[\Delta t]^8, \quad (81)$$

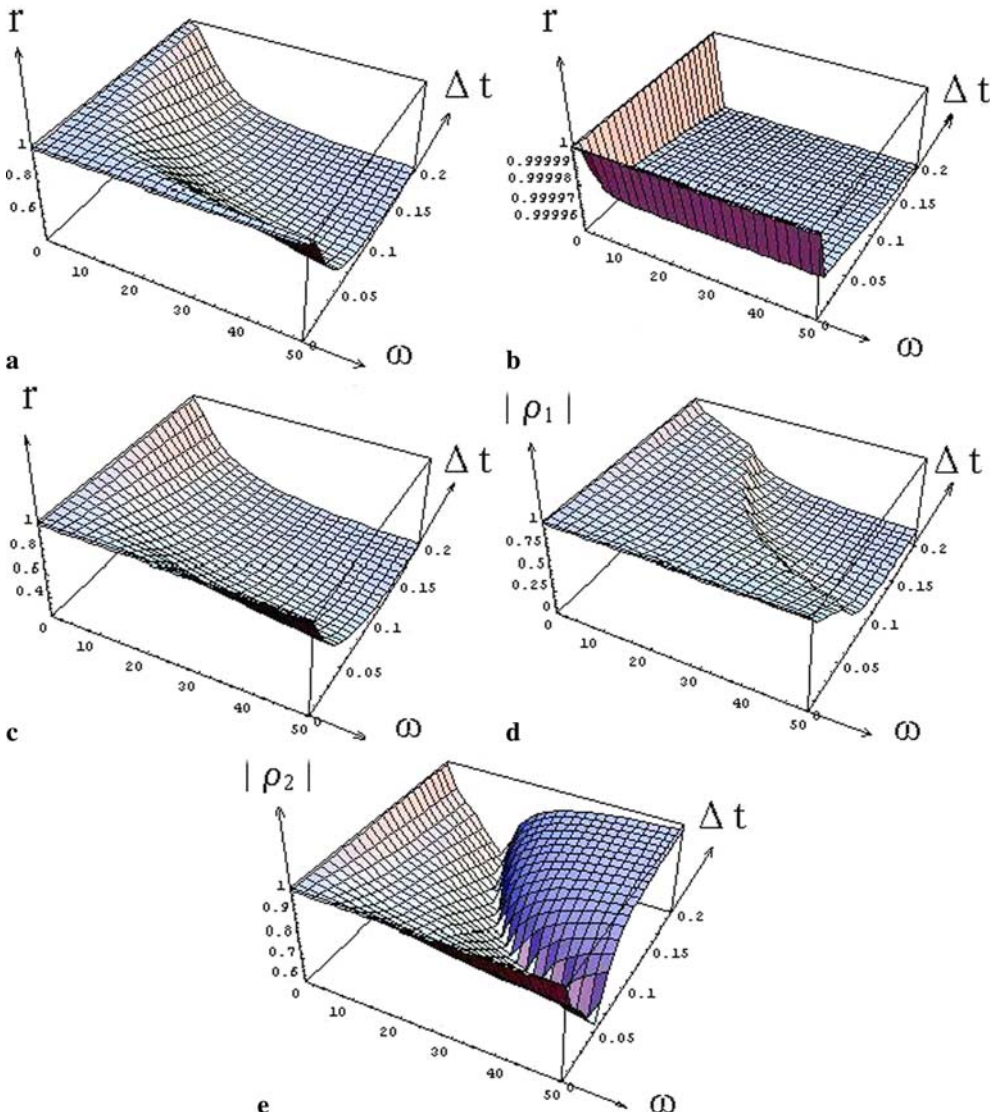

Fig. 3 Spectral radii r and absolute values of two eigenvectors ρ_1 and ρ_2 of the numerical amplification matrix for the TCG method with quadratic approximations in time and the predictor/multi-corrector solver with two iterations. **(a)** r at $a = 0.001, \gamma_3 = 2$ and $\xi = 0$; **(b)** r at $a = 1,000$, $\gamma_3 = 20,000$ and $\xi = 0$; **(c)** r at $a = 0.001, \gamma_3 = 2$ and $\xi = 0.3$; **(d, e)** ρ_1 and ρ_2 at $a = 1,000, \gamma_3 = 2$ and $\xi = 0.3$

$$A_{12} = -A_{21}/\omega^2 = \cdots + [\omega^3(a\omega - 32a^2\xi^5\omega^2 - 21a^3\omega^3 + 1344a^3\xi^6\omega^3 + \xi(4 - 6a^2\omega^2) + 8\xi^3(-1 + 4a^2\omega^2) + 12a\xi^2\omega(-1 + 42a^2\omega^2) + \xi^4(16a\omega - 1680a^3\omega^3))\Delta t^7]/100800a^3 + O[\Delta t]^8. \quad (82)$$

The spectral radii $r = r(\Omega, \alpha, \xi)$ of the numerical matrix $[A]$ are given in Fig. 4. It is necessary to mention that at $\xi = 0$ and $\alpha \neq 0$ the spectral radius r is greater than unity at small values of Ω. We can not see this fact from Fig. 4 because this value ($r > 1$) is close to unity for a very narrow range of the parameter Ω. However, the spectral radius r is smaller or equal to unity if $\alpha = 0$ (at very large values of the parameter a) or if small physical damping is introduced, e.g., $r \leq 1$ at $\xi = 0.001$ and $0 \leq \alpha \leq 10$ or at $\xi = 0.005$ and $0 \leq \alpha \leq 1000$. The modification of the method with $\alpha = 0$ and $\lambda_{1,2}(t) \neq 1$ and without the introduction of the physical damping ξ, considered in our paper (A.V. Idesman, submitted), allows for the unconditionally stable method of the sixth order of accuracy with numerical dissipation at high frequencies (we do not consider the case $\lambda_{1,2}(t) \neq 1$ in this paper).

2.8.2 *The predictor/multi-corrector solver (without damping)*

We will analyze the amplification matrix $[A]$ after three iterations with only one correction of the vector $\boldsymbol{U}_2$ [see

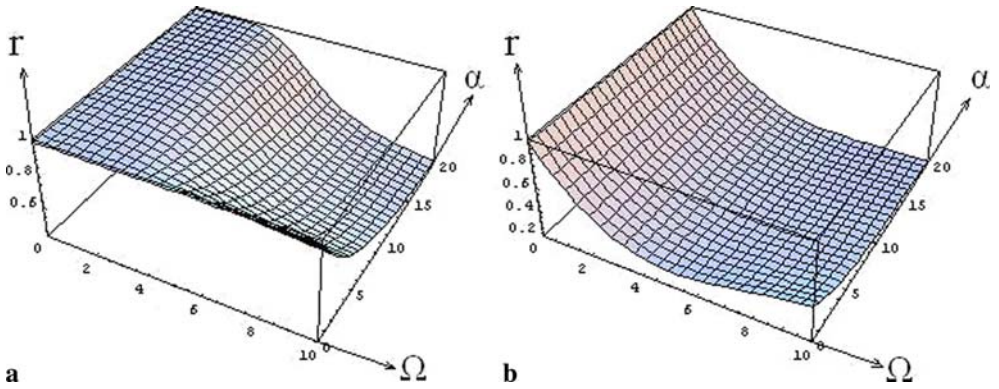

Fig. 4 Spectral radii r for the TCG method with third-order approximations in time and a direct solver for $\xi = 0$ (**a**) and $\xi = 0.3$ (**b**)

Eqs. (54), (55) and (59)]. The following representations of the parameters $\gamma_1 = 0$ and $\gamma_2 = \gamma_3 \Delta t^3$ in Eq. (58) are used for the analysis (γ_3 is a new parameter). The highest-order terms in the expansion of the elements of the matrix $[A]$ into the Taylor series, which differ from Eqs. (63)–(65), are given below:

$$A_{11} = \cdots + \frac{(\omega^4 - a^2\omega^6)\Delta t^7}{100800a^3} + O[\Delta t]^8, \tag{83}$$

$$A_{22} = \cdots + \frac{(\omega^4 - a^2\omega^6)\Delta t^7}{100800a^3} + O[\Delta t]^8, \tag{84}$$

$$A_{12} = \frac{(\omega^4 - 21a^2\omega^6)\Delta t^7}{100800a^2} + O[\Delta t]^8, \tag{85}$$

$$A_{21} = -\frac{(\omega^6 - 105a^2\omega^8)\Delta t^7}{100800a^2} + O[\Delta t]^8. \tag{86}$$

Because the eigenvalues of the numerical amplification matrix $[A]$ are not always complex conjugate, we will present absolute values of two eigenvectors ρ_1 and ρ_2 (see Fig. 5).

2.8.3 *The predictor/multi-corrector solver (with damping)*

We will analyze the amplification matrix $[A]$ after three iterations [see Eqs. (54) -(57)]. The following representations of the parameters $\gamma_1 = 0$ and $\gamma_2 = \gamma_3 \Delta t^3$ in Eq. (58) are used for the analysis (γ_3 is a new parameter). The highest-order terms in the expansion of the elements of the matrix $[A]$ into the Taylor series, which differ from Eqs. (63)–(65), are given below:

$$\begin{aligned} A_{11} = \cdots + [&(\omega^4(1 - a^2\omega^2 - 16a^2\xi^4\omega^2 + 672a^3\xi^5\omega^3 \\ &+ 4\xi^2(-1 + 3a^2\omega^2) + 2a\xi\omega(-2 + 63a^2\omega^2) \\ &+ \xi^3(8a\omega - 672a^3\omega^3))\Delta t^7]/100800a^3 + O[\Delta t]^8, \end{aligned} \tag{87}$$

$$\begin{aligned} A_{22} = \cdots + [&(\omega^4(1 - a^2\omega^2 + 64a^2\xi^6\omega^2 - 26880a^3\xi^7\omega^3 \\ &+ \xi^4(16 - 80a^2\omega^2) + 12\xi^2(-1 + 2a^2\omega^2) \\ &+ 6a\xi\omega(-1 + 84a^2\omega^2) + 32a\xi^5\omega(-1 + 147a^2\omega^2) \\ &+ \xi^3(32a\omega - 3360a^3\omega^3))\Delta t^7)]/100800a^3 + O[\Delta t]^8 \end{aligned} \tag{88}$$

$$\begin{aligned} A_{12} = \cdots + [&(\omega^3(a\omega - 32a^2\xi^5\omega^2 - 21a^3\omega^3 \\ &+ 1344a^3\xi^6\omega^3 + \xi(4 - 6a^2\omega^2) + 8\xi^3(-1 + 4a^2\omega^2) \\ &+ 12a\xi^2\omega(-1 + 42a^2\omega^2) \\ &+ \xi^4(16a\omega - 1680a^3\omega^3))\Delta t^7)]/100800a^3 + O[\Delta t]^8, \end{aligned} \tag{89}$$

$$\begin{aligned} A_{21} = \cdots + [&(\omega^5(a\omega - 32a^2\xi^5\omega^2 - 105a^3\omega^3 \\ &+ 13440a^3\xi^6\omega^3 + \xi(4 - 6a^2\omega^2) + 8\xi^3(-1 + 4a^2\omega^2) \\ &+ 12a\xi^2\omega(-1 + 126a^2\omega^2) \\ &+ 16\xi^4(a\omega + 63a^3\omega^3))\Delta t^7)]/100800a^3 + O[\Delta t]^8. \end{aligned} \tag{90}$$

Because the eigenvalues of the numerical amplification matrix $[A]$ are not always complex conjugate, we will present absolute values of two eigenvectors ρ_1 and ρ_2 (see Fig. 6).

From the analysis of the amplification matrix $[A]$ presented above, it follows that at linear, quadratic and third-order time approximations for displacements and velocities, the new TCG method has the second, fourth and sixth order of accuracy, respectively. It means that the accuracy of the new implicit TCG method is increased by a factor of two in comparison to that of the standard TCG method [3] and is one order higher than the accuracy of the standard TDG method [12–15,17,18] (and the high-order accurate methods suggested in [6,21]) at the same number of degrees of freedom (see Table 1). The new method is unconditionally stable (spectral radii are $r \leq 1$ for both the direct solver and the predictor/multi-corrector solvers) and has controllable numerical dissipation.

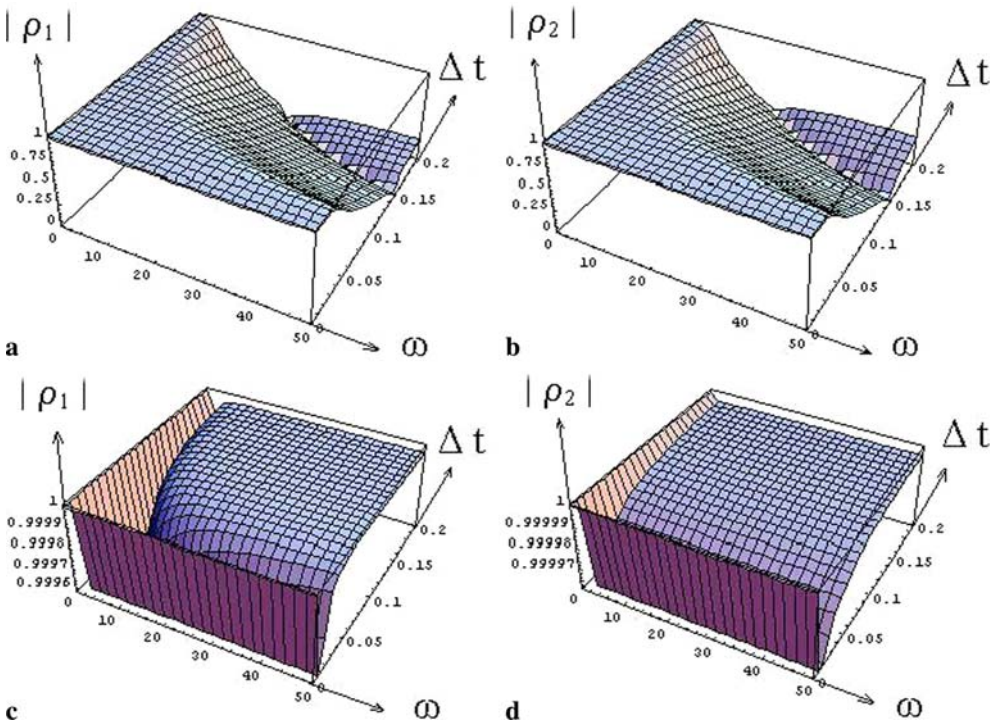

Fig. 5 Absolute values of two eigenvectors ρ_1 and ρ_2 of the numerical amplification matrix for the TCG method with third-order approximations in time and the predictor/multi-corrector solver with three iterations (without damping, $\xi = 0$). **(a, b)** $a = 0.001$ and $\gamma_3 = 10$; **(c, d)** $a = 1,000$ and $\gamma_3 = 2 \cdot 10^6$

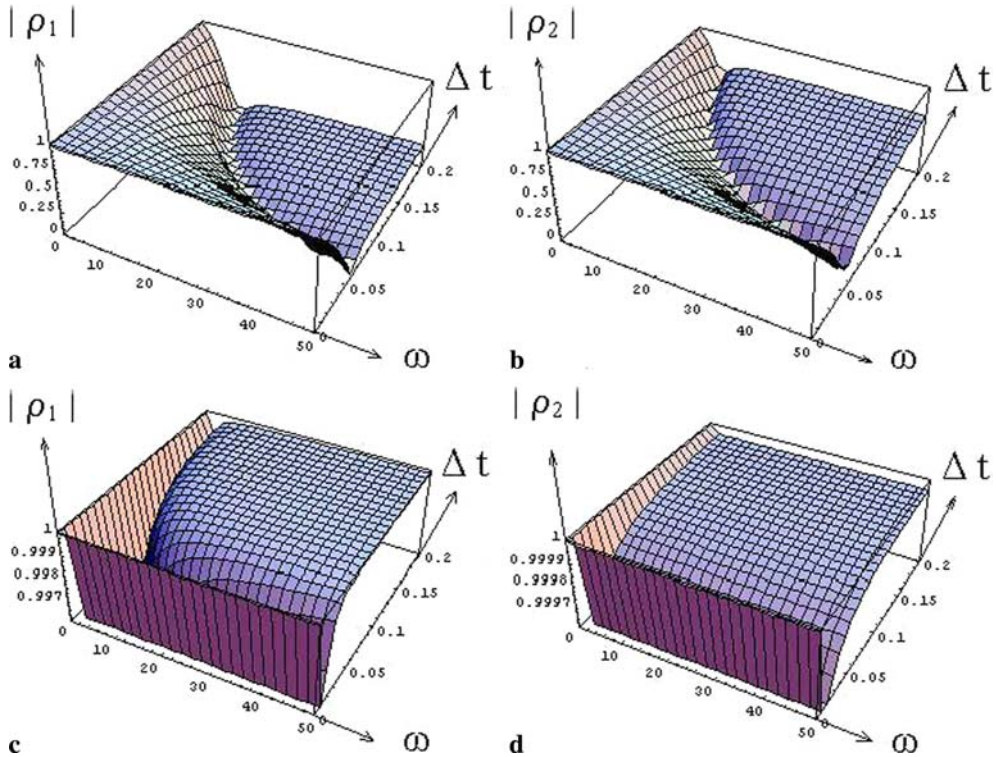

Fig. 6 Absolute values of two eigenvectors ρ_1 and ρ_2 of the numerical amplification matrix for the TCG method with third-order approximations in time and the predictor/multi-corrector solver with three iterations (with damping, $\xi = 0.3$). **(a, b)** $a = 0.001$ and $\gamma_3 = 20$; **(c, d)** $a = 1,000$ and $\gamma_3 = 2 \cdot 10^5$

Table 1 Accuracy of TCG and TDG methods for elastodynamics (the number of unknowns for TCG and TDG methods is reduced by a factor of two due to analytical transformations)

Number of degress of freedom	New TCG (with control of high frequencies)		Standard TCG (no control of high frequencies)		Standard TDG (no control of high frequencies)	
	Order of accuracy in time	Time approximations	Order of accuracy in time	Time approximations	Order of accuracy in time	Time approximations
m	2	Linear ($n = 1$)	1	Linear		
2m	4	Quadratic ($n = 2$)	2	Quadratic	3	Linear
3m	6	Third order ($n = 3$)	3	Third order	5	Quadratic

m is the number of unknowns for known second-order accurate methods

For direct solvers and the case without physical damping $\xi = 0$, the decrease in the parameter a (or the increase in the parameter α) leads to the decrease in the spectral radii at high frequencies for all time approximations of displacements and velocities; for $\alpha \to 0$ (or very large values of the parameter a) the spectral radius tends to one at all frequencies (no numerical dissipation) (see Figs. 1, 2 and 4). It means that numerical dissipation at high frequencies increases with the decrease in a. For the predictor/multi-corrector solver the eigenvalues of the amplification matrix $[A]$ are not always complex conjugate; i.e., two different eigenvectors ρ_1 and ρ_2 of the matrix $[A]$ can exist at the same Δt and ω (see Figs. 3, 5 and 6). From the analysis presented it can be seen that the effective mass matrix does not necessarily need to include the damping matrix $\boldsymbol{C}$ [see Eqs. (33) and (58)]. In this case, small values of the parameter γ_3 lead to the increase in numerical dissipation; large values of the parameter γ_3 lead to the decrease in numerical dissipation (see Figs. 3, 5 and 6). In contrast to the standard TDG method, which does not have parameters changing numerical dissipation, the new TCG method allows the variation of the numerical dissipation. The importance of this property can be seen from the numerical examples considered below.

3 A new strategy to solution of elastodynamics problems

In [10] several important attributes of competitive numerical methods for elastodynamics are discussed. It is known that due to spatial finite element discretization the exact solution of a discrete problem differs from the exact solution of the continuous problem by the inclusion of spurious high-frequency oscillations. Therefore, controllable algorithmic dissipation in higher modes is an important property of any numerical method for elastodynamics [10]. This numerical dissipation damps out spurious high-frequency oscillations. Numerical methods that do not possess this property are not considered as competitive ones. Here, we are going to present a new strategy that will allow the effective use of high-order accurate methods with zero or very small numerical dissipation.

As it was indicated above, the integration of a system of semi-discrete elastodynamics Eqs. (2) can be reduced to the time integration of n independent ordinary differential equations of the form of Eqs. (60)–(61) where n is the number of modes (see [10]). Usually, the accurate time integration of equations with low modes and the damping out of equations containing high modes are required. This result can be achieved by a method with controllable numerical dissipation. The idea of the new strategy is very simple. The basic computations, especially for a long-term integration, can be done by a high-order method with zero or very small numerical dissipation. It means that all modes are integrated very accurately. Then, for the damping out of high modes, a method with large numerical dissipation can be used for a number of last time increments or as a post-processor. This method can be considered as a filter of high modes. It should be mentioned that the use of a method with large numerical dissipation at high modes for all time increments leads to accumulation of a numerical error for low-mode terms as well, especially at the long-term integration. Therefore, a new strategy will be much more effective and accurate for a long-term solution. The proposed high-order accurate TCG methods with zero or small dissipation for basic computations and the second-oder TCG method with large numerical dissipation for the final time increments can be used for the new approach. In the case of monitoring a numerical solution at different time moments, the new strategy can be applied repeatedly; i.e., basic computations can be made with a high-order method with zero or very small numerical dissipation, and a number of time increments before specific time moments can be computed by a method with large numerical dissipation. An example of the application of the new strategy to linear problems

is considered below. The application of the new computational strategy to non-linear elastodynamics problems will be considered elsewhere.

4 Numerical examples

The new technique is implemented into the finite element code FEAP [27] by the use of a direct solver. The implementation of the technique by the use of the predictor/multi-corrector iterative procedure will be considered elsewhere.

4.1 Harmonic response of an elastic rod

An elastic rod of the length $L = 1$ is considered. Both ends of the rod are fixed ($u(0,t) = v(0,t) = u(1,t) = v(1,t) = 0$), no external loads are applied, the initial velocity is zero ($v(x,0) = 0$), and the initial displacement is proportional to the first harmonic ($u_0(x,0) = \sin(\pi x)$) (see Fig. 7a). Zero damping is assumed ($\boldsymbol{C} = \boldsymbol{0}$). The observation time is assumed to be $T = 2$; the Young's modulus is $E = 1$, and the density is $\rho = 1$. It is usually impossible to use a uniform mesh for a complicated geometry in the multi-dimensional case. Therefore, to study the effectiveness of the new method, a non-uniform mesh with 100 quadratic finite elements along the bar is used (see Fig. 7b). The element Courant number $Co = c\,\Delta t/\Delta x$ varies along the bar with $Co_{\max}/Co_{\min} = \Delta x_{\max}/\Delta x_{\min} = 7.2$ for any time increment Δt, where $c = 1$ is the wave velocity, and $Co_{\max}$ and $Co_{\min}$ are the maximum and minimum element Courant numbers, respectively. The problem was solved using the linear ($n = 1$), quadratic ($n = 2$) and third order ($n = 3$) time approximations for displacements and velocities, and uniform time increments. The scalar parameter $a = 1,000$ was chosen, and therefore, spectral radii of the amplification matrix were close to unity for all methods with $n = 1,2,3$. To study the convergence of the method, different numbers of time increments (from 2 to 360) were used for the time interval $0 \le t \le 2$. The problem has the continuous analytical solution $u_a(x,t) = \sin(\pi x)\cos(\pi t)$. For the comparison of the accuracy of numerical results, the following error e in the L^2 norm for displacements and velocities at time $t = T = 2$ was calculated:

$$e = \left\{ \int_0^L \{[u_a(x,T) - u_n(x,T)]^2 + [v_a(x,T) - v_n(x,T)]^2\}\,\mathrm{d}x \right\}^{1/2}, \tag{91}$$

where $u_n(x,T)$ and $v_n(x,T)$ are numerical solutions for displacements and velocities at time $T = 2$ ($u_a(x,T = 2) = \sin(\pi x)$, $v_a(x,T = 2) = 0$.

The accuracy of the numerical solution of the problem using the new TCG method is given in Fig. 7c. The problem was solved on the non-uniform mesh shown in Fig. 7b. with the linear, quadratic and third-order time approximations for displacements and velocities, and a different number N of time increments. The computation time is proportional to N. It is also necessary to note that the numerical solution with the classical trapezoidal rule (the second-order method with no numerical dissipation) coincides with curve 1 in Fig. 7c. From these results it follows that at the same accuracy, the method with the second order of accuracy requires from 20 (at accuracy $\log e = -3$) to 100 (at accuracy $\log e = -6$) times more time increments than, for example, the new TCG method with the fourth order of accuracy does (see curves 1 and 2 in Fig. 7c). It means that the use of the new fourth-order accurate TCG method for this simple problem reduces the computation time by a factor 5–25 or more in comparison to that for the second-order method (here we took into account that for one time increment the fourth-order TCG method requires four times as much computation time as the second-order method). To compare the new TCG method and the standard TDG method, we solved the problem by the TDG method with quadratic time approximations for displacements and velocities (curve 4). The numbers of degrees of freedom for the TDG method (curve 4) and the new TCG method with the third order of time approximations (curve 3) are the same. However, comparing curves 3 and 4 at the same accuracy ($\log e = -2/-5$), we can conclude that for the problem under consideration, the new TCG method is much faster than the standard TDG method. No numerical dissipation is necessary for this problem. The new TCG method with $a = 1000$ has almost zero dissipation (see Figs. 1, 2 and 4). Numerical dissipation of the TDG method diminishes the accuracy of the numerical solution (the standard TDG method does not have a parameter that can change the numerical dissipation). The reduction in the computation cost with the new TCG method will be more essential for 2-D and 3-D problems with a large number of degrees of freedom.

4.2 Impact of an elastic bar against a rigid wall

The second example is related to impact against a rigid wall of an elastic bar of the length $L = 4$ (see Fig. 8a). The right end of the rod is fixed ($u(4,t) = v(4,t) = 0$), the velocity $v = 1$ is instantly applied at the left end ($u(0,t) = t, v(0,t) = 1$), and the initial displacements and

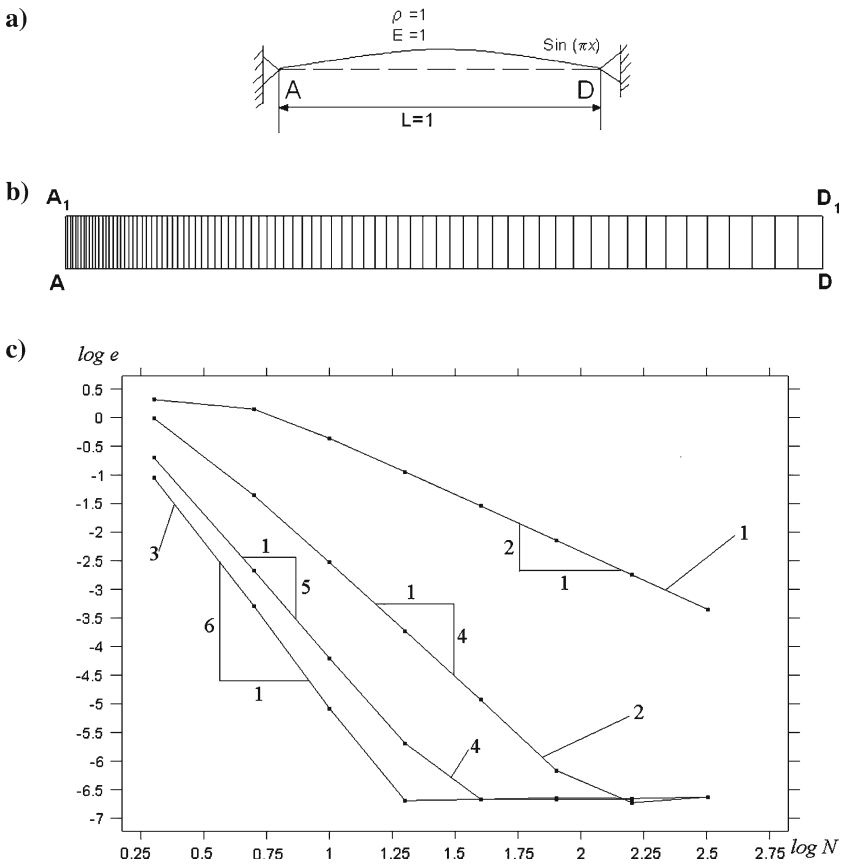

Fig. 7 Harmonic response of an elastic rod (**a**). The mesh for each time increment consists of 100 non-uniform quadratic elements along the x-axis (**b**). A numerical error e at time $T = 2$ for the new TCG method with the linear (curve 1), quadratic (curve 2) and third-order (curve 3) time approximations, and for the standard TDG method with quadratic time approximations (curve 4) (**c**)

velocities are zero. Zero damping is assumed ($\boldsymbol{C} = \boldsymbol{0}$). The observation time T is chosen to be $T = 2.8$; the Young's modulus is $E = 1$, and the density is $\rho = 1$. The problem was solved with 100 non-uniform linear finite elements shown in Fig. 7b (with $AD = L = 4$). The problem has the continuous solution for displacements $u_a(x,t) = t - x$ for $t \geq x$ and $u_a(x,t) = 0$ for $t \leq x$, and the discontinuous solution for velocities and stresses $v_a(x,t) = -\sigma^a(x,t) = 1$ for $t \geq x$ and $v_a(x,t) = \sigma^a(x,t) = 0$ for $t \leq x$ (at the interface $x = t$ jumps in stresses and velocities occur).

It is known that the application of the traditional semi-discrete methods to this problem leads to oscillations in velocities and stresses due to the spurious high-frequency response (see [12,15]). The standard TDG method (e.g., see [4,15,20,24]) also yields spurious oscillations for this problem, especially on non-uniform meshes in space (see our results in Fig. 8b). In [12,15] the special non-linear formulations, with the discontinuity-capturing operators based on the TDG method, were developed to exclude the spurious response. However, numerical results show that for the new TCG method with linear elements (which has the second order of accuracy in time), the spurious oscillations can be excluded. As can be seen from Fig. 1, spectral moduli at high frequencies decrease with the increase in the parameter α (the decrease in the absolute value of the scalar a in Eqs. (5)–(7)) and with the increase in the parameter Ω. The decrease in the spectral moduli leads to the increase in the numerical dissipation of the new TCG method and the suppression of spurious oscillations. The solution with the new TCG at time $T = 2.8$ (linear approximations of displacements and velocities in time, and 160 uniform time increments $\Delta t = 0.0175$ were used) corresponds to the smooth curve 1 in Fig. 8c with no spurious oscillations. The numerical results show that the use of higher-order time approximations for displacements and velocities yields a few oscillations for velocities at any value of a and Δt (or the Courant number). However, the new strategy combining high-order accurate methods with zero or small dissipation for basic computations and a method with large numerical dissipation for last time increments yields an accurate solution with no spurious high-frequency oscillations. For example, curve 2 in Fig. 8c corresponds to the solution at time $T = 2.8$ for the first 30 uniform time increments $\Delta t = 0.07$ with quadratic approximations of displacements and velocities in time, and $a = 100$; and the last

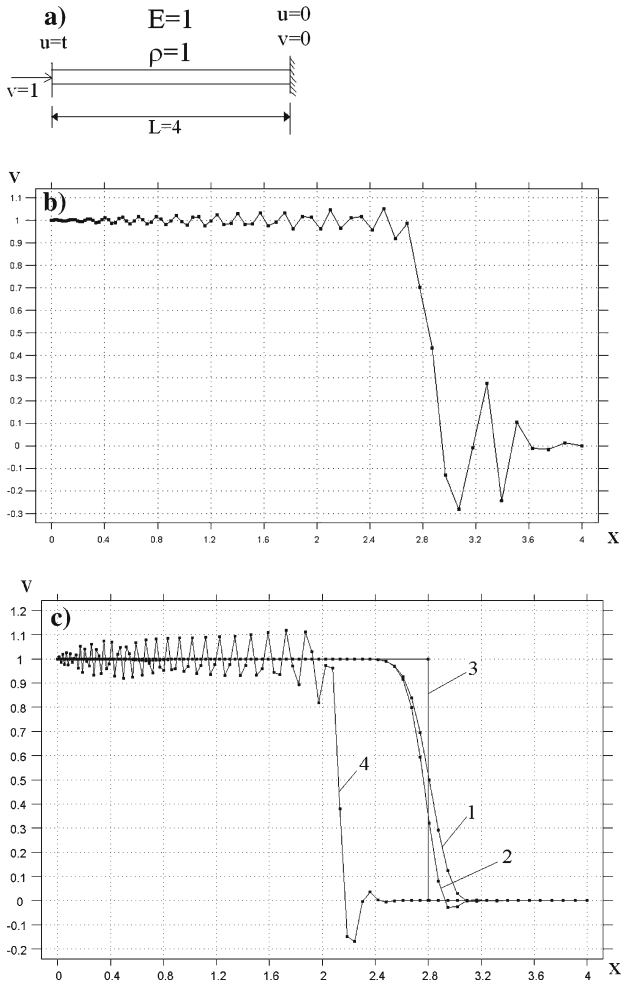

Fig. 8 Impact of an elastic bar against a rigid wall (**a**). Velocity distribution along the bar at time $T = 2.8$ computed on the non-uniform mesh containing 100 linear elements (see Fig. 7b) using the standard TDG method (**b**) and the new TCG method (**c**). For the TCG method (**c**) curves 1, 2, 3, and 4 correspond to: the solution with linear time approximations, 160 uniform time increments $\Delta t = 0.0175$ and $a = 0.001$; the solution obtained after the first 30 uniform time increments $\Delta t = 0.07$ with quadratic time approximations and $a = 1000$ (see curve 4), and the last 40 uniform time increments $\Delta t = 0.0175$ with linear time approximations and $a = 0.001$; the analytical solution; and the solution with quadratic time approximations, 30 uniform time increments $\Delta t = 0.07$ ($T = 2.1$) and $a = 1000$, respectively

40 uniform time increments $\Delta t = 0.0175$ with linear approximations of displacements and velocities in time, $a = 0.001$ and $\lambda_1 = \lambda_2 = 1 + 10^{10}t^4$ [see Eq. (3)]. The introduction of weighting functions λ_1 and λ_2 allows the addition of numerical dissipation without an effect on the accuracy of the method (A.V. Idesman, submitted). It can be seen from Fig. 8c that the last 40 time increments allow the suppression of spurious oscillations after the first 30 time increments, curve 4. Despite the fact that the first 30 time increments are larger than the last 40 time increments, the solution combining high-order accurate non-dissipative and dissipative methods (curve 2) yields a steeper curve than the solution by the TCG method with linear time approximations, 160 uniform time increments, and $a = 0.001$ (see curve 1).

Remark It is interesting to note that the modified TDG method with the new weighting functions λ_1 and λ_2 suggested in (A.V. Idesman, submitted) allows the solution of the considered problem with no spurious oscillations for linear approximations of displacements and velocities in time.

5 Concluding remarks

A new high-order accurate TCG method for elastodynamics is suggested. The new method is unconditionally stable and has controllable numerical dissipation at high frequencies. The main advantages of the new method are the higher order of accuracy in comparison to that of known high-order accurate methods (if the same number of degrees of freedom is used) and controllable numerical dissipation. However, even methods with zero or small numerical dissipation can be very effectively used for wave propagation problems with the application of the new suggested strategy for the solution of elastodynamics problems. This strategy consists in the combination of numerical methods with small and large numerical dissipation where the latter can be used for a number of last time increments or as a post-processor. Simple 1-D numerical tests show a significant reduction in the computation time (by 5–25 times) for the new method with a direct solver in comparison to that for second-order methods, and the suppression of spurious high-frequency oscillations. The reduction in the computation time will be more essential for 2-D and 3-D problems with the suggested predictor/multicorrector solver that requires few iterations in order to reach the accuracy of direct solvers. This study as well as the application of the new TCG method and new numerical strategy to non-linear problems will be considered in the future.

Acknowledgements The author gratefully acknowledges the support of Texas Tech University.

Appendix: Explicit expressions for the coefficients b_{ij}, d_{ij} and f_{ij}

(a) Quadratic time approximations of displacements and velocities.

$$\begin{bmatrix} b_{11} & b_{12} \\ b_{21} & b_{22} \end{bmatrix} = \begin{bmatrix} -\dfrac{2(24a^2+9a\Delta t+\Delta t^2)}{3(20a^2+12a\Delta t+3\Delta t^2)} & 2a+\Delta t \\ -\dfrac{(40a^3+36a^2\Delta t+10a\Delta t^2+\Delta t^3)}{\Delta t(20a^2+12a\Delta t+3\Delta t^2)} & \frac{2(3a+\Delta t)}{3} \end{bmatrix}; \begin{bmatrix} d_{11} & d_{12} & d_{13} & d_{14} \\ d_{21} & d_{22} & d_{23} & d_{24} \end{bmatrix}$$

$$= \begin{bmatrix} a+\frac{\Delta t}{2} & \frac{1}{3}\Delta t(3a+2\Delta t) & \frac{1}{6}\Delta t(3a+2\Delta t) & \frac{1}{12}\Delta t^2(4a+3\Delta t) \\ a+\frac{\Delta t}{3} & \frac{1}{6}\Delta t(8a+3\Delta t) & \frac{1}{12}\Delta t(8a+3\Delta t) & \frac{1}{10}\Delta t^2(5a+2\Delta t) \end{bmatrix}; \begin{bmatrix} f_{11} & f_{12} & f_{13} & f_{14} & f_{15} & f_{16} \\ f_{21} & f_{22} & f_{23} & f_{24} & f_{25} & f_{26} \end{bmatrix}$$

$$= \begin{bmatrix} 0 & \dfrac{2(24a^2+9a\Delta t+\Delta t^2)}{3(20a^2+12a\Delta t+3\Delta t^2)} & 0 & 0 & a+\frac{\Delta t}{2} & 0 \\ 0 & \dfrac{40a^3+36a^2\Delta t+10a\Delta t^2+\Delta t^3}{\Delta t(20a^2+12a\Delta t+3\Delta t^2)} & 0 & 0 & a+\frac{\Delta t}{3} & 0 \end{bmatrix}.$$

(b) Third-order time approximations of displacements and velocities.

$$\begin{bmatrix} b_{11} & b_{12} & b_{13} \\ b_{21} & b_{22} & b_{23} \\ b_{31} & b_{32} & b_{33} \end{bmatrix} = \begin{bmatrix} \dfrac{5(336a^4+336a^3\Delta t+108a^2\Delta t^2+16a\Delta t^3+\Delta t^4)}{8\Delta t(105a^3+60a^2\Delta t+15a\Delta t^2+2\Delta t^3)} & 2a+\Delta t & \Delta t(3a+2\Delta t) \\ \dfrac{420a^4+390a^3\Delta t+120a^2\Delta t^2+17a\Delta t^3+\Delta t^4}{2\Delta t(105a^3+60a^2\Delta t+15a\Delta t^2+2\Delta t^3)} & \frac{2}{3}(3a+\Delta t) & \frac{1}{2}\Delta t(8a+3\Delta t) \\ \dfrac{630a^4+480a^3\Delta t+135a^2\Delta t^2+18a\Delta t^3+\Delta t^4}{2\Delta t(105a^3+60a^2\Delta t+15a\Delta t^2+2\Delta t^3)} & \frac{1}{2}(4a+\Delta t) & \frac{3}{10}\Delta t(15a+4\Delta t) \end{bmatrix};$$

$$\begin{bmatrix} d_{11} & d_{12} & d_{13} & d_{14} & d_{15} & d_{16} \\ d_{21} & d_{22} & d_{23} & d_{24} & d_{25} & d_{26} \\ d_{31} & d_{32} & d_{33} & d_{34} & d_{35} & d_{36} \end{bmatrix}$$

$$= \begin{bmatrix} a+\frac{\Delta t}{2} & \frac{1}{3}\Delta t(3a+2\Delta t) & \frac{1}{4}\Delta t^2(4a+3\Delta t) & \frac{1}{6}\Delta t(3a+2\Delta t) & \frac{1}{12}\Delta t^2(4a+3\Delta t) & \frac{1}{20}\Delta t^3(5a+4\Delta t) \\ a+\frac{\Delta t}{3} & \frac{1}{6}\Delta t(8a+3\Delta t) & \frac{3}{10}\Delta t^2(5a+2\Delta t) & \frac{1}{12}\Delta t(8a+3\Delta t) & \frac{1}{10}\Delta t^2(5a+2\Delta t) & \frac{1}{30}\Delta t^3(12a+5\Delta t) \\ a+\frac{\Delta t}{4} & \frac{1}{10}\Delta t(15a+4\Delta t) & \frac{1}{10}\Delta t^2(18a+5\Delta t) & \frac{1}{20}\Delta t(15a+4\Delta t) & \frac{1}{30}\Delta t^2(18a+5\Delta t) & \frac{1}{14}\Delta t^3(7a+2\Delta t) \end{bmatrix};$$

$$\begin{bmatrix} f_{11} & f_{12} & f_{13} & f_{14} & f_{15} & f_{16} \\ f_{21} & f_{22} & f_{23} & f_{24} & f_{25} & f_{26} \\ f_{31} & f_{32} & f_{33} & f_{34} & f_{35} & f_{36} \end{bmatrix} = \begin{bmatrix} 0 & -\dfrac{5(336a^4+336a^3\Delta t+108a^2\Delta t^2+16a\Delta t^3+\Delta t^4)}{8\Delta t(105a^3+60a^2\Delta t+15a\Delta t^2+2\Delta t^3)} & 0 & 0 & a+\dfrac{\Delta t}{2} & 0 \\ 0 & -\dfrac{420a^4+390a^3\Delta t+120a^2\Delta t^2+17a\Delta t^3+\Delta t^4}{2\Delta t(105a^3+60a^2\Delta t+15a\Delta t^2+2\Delta t^3)} & 0 & 0 & a+\dfrac{\Delta t}{3} & 0 \\ 0 & -\dfrac{630a^4+480a^3\Delta t+135a^2\Delta t^2+18\Delta t^3+\Delta t^4}{2\Delta t(105a^3+60a^2\Delta t+15a\Delta t^2+2\Delta t^3)} & 0 & 0 & a+\frac{\Delta t}{4} & 0 \end{bmatrix}.$$

References

1. Bonelli A, Bursi OS (2001) Explicit predictor-multicorrector time discontinuous galerkin methods for linear dynamics. J Sound Vib 246(4):625–652
2. Bonelli A, Bursi OS (2003) Iterative solutions for implicit time discontinuous galerkin methods applied to non-linear elastodynamics. Comput Mech 30(5-6):487–498
3. Cannarozzi M, Mancuso M (1995) Formulation and analysis of variational methods for time integration of linear elasto-dynamics. Comput Methods Appl Mech Eng 127(1-4):241–257
4. Chien CC, Wu TY (2000) Improved predictor/multi-corrector algorithm for a time-discontinuous galerkin finite element method in structural dynamics. Comput Mech 25(5):430–437

5. Chien CC, Yang CS, Tang TH (2003) Three-dimensional transient elastodynamic analysis by a space and time-discontinuous galerkin finite element method. Finite Elem Anal Des 39(7):561–580
6. Fung TC (2005) Construction of higher-order accurate time-step integration algorithms by equal-order polynomial projection. J Vib Control 11(1):19–49
7. Hilber HM, Hughes TJR (1978) Collocation, dissipation and 'overshoot' for time integration schemes in structural dynamics. Earthquake Engrg Struct Dyn (6):99–118
8. Hilber HM, Hughes TJR, Taylor RL (1977) Improved numerical dissipation for time integration algorithms in structural dynamics. Earthquake Eng Struct Dyn (5):283–292
9. Houbolt JC (1950) A recurrence matrix solution for the dynamic response of elastic aircraft. J Aeronaut Sci (17):540–550
10. Hughes TJR (1987) The finite element method: linear static and dynamic finite element analysis. Prentice- Hall, Englewood Cliffs
11. Hughes TJR, Hulbert GM (1988) Space-time finite element methods for elastodynamics: Formulations and error estimates. Comput Methods Appl Mech Eng 66(3):339–363
12. Hulbert GM (1992) Discontinuity-capturing operators for elastodynamics. Comput Methods Appl Mech Eng 96(3):409–426
13. Hulbert GM (1992) Time finite element methods for structural dynamics. Inter J Numer Methods Eng 33(2):307–331
14. Hulbert GM (1994) A unified set of a single-step asymptotic annihilation algorithms for structural dynamics. Comput Methods Appl Mech Eng 113:1–9
15. Hulbert GM, Hughes TJR (1990) Space-time finite element methods for second-order hyperbolic equations. Comput Methods Appl Mech Eng 84(3):327–348
16. Kim SJ, Cho JY, Kim WD (1997) From the trapezoidal rule to higher-order accurate and unconditionally stable time-integration method for structural dynamics. Comput Methods Appl Mech Eng 149(1-4):73–88
17. Kunthong P, Thompson LL (2005) An efficient solver for the high-order accurate time-discontinuous galerkin (tdg) method for second-order hyperbolic systems. Finite Elem Anal Des 41(7-8):729–762
18. Li XD, Wiberg NE (1996) Structural dynamic analysis by a time-discontinuous galerkin finite element method. Int J Numer Methods Eng 39(12):2131–2152
19. Li XD, Wiberg NE (1998) Implementation and adaptivity of a space-time finite element method for structural dynamics. Comput Methods Appl Mech Eng 156:211–229
20. Mancuso M, Ubertini F (2003) An efficient integration procedure for linear dynamics based on a time discontinuous galerkin formulation. Comput Mech 32(3):154–168
21. Mancuso M, Ubertini F (2003) A methodology for the generation of low-cost higher-order methods for linear dynamics. Int J Numer Methods Eng 56(13):1883–1912
22. Newmark NM (1959) A method of computation for structural dynamics. J Eng Mech Div ASCE 85:67–94
23. Park KC (1975) Evaluating time integration methods for nonlinear dynamic analysis. In: Belytschko T et al. (ed) Finite element analysis of transient nonlinear behavior, AMD 14, ASME, New York, pp 35–58
24. Thompson LL, He D (2005) Adaptive space-time finite element methods for the wave equation on unbounded domains. Comput Methods Appl Mech Eng 194(18-20):1947–2000
25. Wiberg NE, Li XD (1999) Adaptive finite element procedures for linear and non-linear dynamics. Int J Numer Methods Eng 46(10):1781–1802
26. Wilson EL, Farhoomand I, Bathe KJ (1973) Nonlinear dynamic analysis of complex structures. Earthquake Eng Struct Dyn (1):242–252
27. Zienkiewicz OC, Taylor RL (2000) The finite element method. Butterworth-Heinemann, Oxford, UK
28. Zienkiewicz OC, Wood WL, Hines NW, Taylor RL (1984) Unified set of single step algorithms - part i: General formulation and applications. Int J Numer Methods Eng 20(8):1529–1552